CHALMERS
UNIVERSITY OF TECHNOLOGY

University of Stuttgart
Germany

Cathodic Corrosion Protection in the Context of Lifetime Extension of Monopile-based Offshore Wind Turbines

Master's thesis in Master Programme Sustainable Energy Systems

JUTTA STUTZMANN

Department of Materials and Manufacturing Technology
CHALMERS UNIVERSITY OF TECHNOLOGY
Gothenburg, Sweden 2017

Master's thesis 2017:206

Cathodic Corrosion Protection in the Context of Lifetime Extension of Monopile-based Offshore Wind Turbines

JUTTA STUTZMANN

CHALMERS
UNIVERSITY OF TECHNOLOGY

Department of Materials and Manufacturing Technology
Chalmers University of Technology
Gothenburg, Sweden

RAMBØLL

Wind & Towers (Offshore Wind)
Rambøll Energy
Hamburg, Germany

Bridge and Tunnel Asset Management
Rambøll Transport
Copenhagen, Denmark

Cathodic Corrosion Protection in the Context of Lifetime Extension of Monopile-based Offshore Wind Turbines
JUTTA STUTZMANN

Supervisor	Lisa Ziegler, Rambøll Wind & Towers
Supervisor	Peter H. Møller, Rambøll Bridge and Tunnel Asset Management
Supervisor	Frederik Marthedal Christiansen, Rambøll Bridge and Tunnel Asset Management
Examiner	Mats Norell, Department of Materials and Manufacturing Technology, Chalmers University of Technology
Examiner	Prof. Tekn. Dr. Damian Vogt, Institute of Thermal Turbomachinery and Machinery Laboratory (ITSM), University of Stuttgart

Master's Thesis
Department of Materials and Manufacturing Technology
Chalmers University of Technology
SE-412 96 Gothenburg

Typeset in LaTeX
Printed by Chalmers Reproservice
Gothenburg, Sweden 2017

Cathodic Corrosion Protection in the Context of Lifetime Extension of Monopile-based Offshore Wind Turbines
JUTTA STUTZMANN

Abstract

The first offshore wind farms face the end of their design lifetime in the upcoming years and with that service life extension becomes increasingly important. Offshore wind turbines are exposed to dynamic loads from wind and waves and to harsh environmental offshore conditions. Salt water and humidity abet corrosion on intermittently or completely submerged parts of an offshore support structure; free corrosion decreases the bearable loads. Hence, it is required to evaluate how long existing structures are effectively protected against corrosion.

This thesis investigates a methodology to predict service life of cathodic corrosion protection systems applying on-site measurement data and simulations by means of the software COMSOL Multiphysics®. On-site measurement data of galvanic anode cathodic protection (GACP) systems and impressed current cathodic protection (ICCP) systems are provided from wind farms.
Corrosion models for GACP systems are developed and calibrated to design and environmental data, like seawater and mud conductivity. Kinetic expressions, as simulation input, are iteratively fitted to measured potentials until simulation outcomes match existing potential data. Average current densities and protection potential at the monopile surface are calculated and compared to design and requirements.
Sensitivity studies are applied to address model as well as measurement uncertainties, showing how important precises measurements are to allow on reliable lifetime predictions of cathodic protection systems. Results suggest that, e.g. anode capacity has a strong influence while other parameters have minor impact on the service life of GACP systems.

Furthermore, this thesis indicates how predictions of cathodic protection performance can be applied to estimate on lifetime extension of the support structure of a monopile-based offshore wind turbine.

The applicability of the approach is critically discussed, since results from simulation adjusted by measurements show high uncertainties. Nevertheless, an initial investigation to predict lifetime of corrosion protection systems is given. Improvement of potential measurements and specific environmental data would reduce uncertainties and allow for representative estimations on service life of corrosion protection systems.

Keywords: lifetime extension, corrosion, cathodic protection system, polarization curves, kinetic expression, offshore wind turbines, monopile.

Acknowledgments

Many people have contributed to the success of this thesis with their experiences, ideas, support, and recommendations - practically and mentally. Therefore, I want to give a special gratitude to:

Mats Norell for the guidance on this project from Chalmers side. Thanks to you, to make it possible for me to write my thesis abroad and pushing this project to its scientific value.

Lisa Ziegler, who initiated this project. Lisa, ich möchte dir aufrichtig für Deine tolle Unterstützung danken, dass du Dir immer alle Zeit genommen hast mich zu betreuen und mich wieder in die richtige Richtung zu lenken, nie das Ziel aus den Augen zu verlieren. Dein Support hatte sehr großen Einfluss auf den Erfolg dieser Arbeit und erweckte die Freude am Wissenschaftlichen Arbeiten in mir!

Peter H. Møller, I would like to sincerely thank you for sharing all your knowledge and extensive experiences with me and that you always took the time answering my questions and helping me to eliminate my confusions. You definitely encouraged my fascination on corrosion! **Frederik Marthedal Christiansen**, thank you so much for all the hours you spent to make me award of corrosion simulation models, for all your support from familiarizing with the software to understanding results, and for all the explanations and inspiring discussions.

I would like to thank the **wind park operators** who provided measurement data. And thanks to **Morten Siwertsen from COMSOL support**, who helped solving any programming problems occurred during this thesis.

I would like to thank **Prof. Dr. Damian Vogt** enabling the Double Degree Master's Program with Chalmers University and the **BW Scholarship**, which created social networks all over the world and financially supported my studies abroad.

Finally, I would like to thank all my colleagues who created contacts to wind farm operators or supported in any other ways. I would like to thank the **New Services Department** and the whole **Wind Offshore Department** in Hamburg and last but not least the **Bridge and Tunnel Asset Management Department** in Copenhagen for a great time at Rambøll.

Ein letzter Dank geht an meine **wunderbare Familie**, die immer hinter mir steht und an mich glaubt!

Jutta Stutzmann, Gothenburg, September 2017

Contents

List of Figures

List of Tables

Acronyms

ASTM	American Society for Testing and Materials
BAW	*Bundesamt für Wasserbau (German)* - Federal Waterways Engineering and Research Institute
BSH	*Bundesamt für Seeschifffahrt und Hydrographie (German)* - Federal Maritime and Hydrographic Agency
CA	Corrosion Allowance
COMSOL	COMSOL Multiphysics® - simulation software
CP	Cathodic Protection
DNV	*Det Norske Veritas (Norwegian)* - Norwegian classification society
DNV GL	Merger of *DNV* and *GL* - international classification society
DOF	Degrees of Freedom
DR	Design Report
EO	Expert Opinion (*only in tables*)
FC	Free Corrosion
GACP	Galvanic Anode Cathodic Protection
GL	*Germanischer Llyod* - German classification society
HAT	Highest Astronomical Tide
ICCP	Impressed Current Cathodic Protection
LAT	Lowest Astronomical Tide
LTE	Lifetime Extension (of monopile)
MIC	Microbial Corrosion
ML	Mudline (*only in figures and tables*)
MP	Monopile
MSL	Mean Seawater Level
NACE	National Association of Corrosion Engineers
NORSOK	Norwegian Standard from petroleum industry
OWT	Offshore Wind Turbine
OWF	Offshore Wind Farm
PC	Polarization Curve
PoH	Potential over Height
ROV	Remotely Operated Vehicle
RP	Recommended Practice
RUL	Remaining Useful Lifetime
SN	Stress over Number of cycle
TB	Tower Bottom
TP	Transition Piece
WP	Wind Park
WTG	Wind Turbine Generator
bc	base case
pw	piecewise

Symbols

Latin Symbols	Description	Unit
$log(a)$	Intercept of the x-axis for SN-curve in logarithmic scale	-
A	Surface to protect	m^2
A_c	Tafel slope factor	V
A_{sea}	Submerged MP area	m^2
a	Constant	-
a_{ox}	Chemical activity for oxidation	-
a_{red}	Chemical activity for reduction	-
b	Constant	-
C	Anode current capacity	Ah
c	Cross section periphery	mm
D	Fatigue damage value	-
d	MP wall thickness	mm
d_{ref}	Reference thickness	mm
d_{MP}	Distance between anodes and MP surface	m
E	Potential	V
E_{Al}	(Design) potential of aluminum anode *(input in* COMSOL*)*	V
E_a	Anode potential	V
E_c	Cathode potential	V
E_{Eq}	Equilibrium potential	V
$E_{Eq,Al}$	Equilibrium potential of aluminum	V
E_{Fe}	Iron potential (*here also potential of the steel surface*)	V
E_{corr}	Corrosion potential	V
E_{red}	Potential at reduction reaction	V
e	Electron	-
F	Faraday constant	$\frac{As}{mol}$
f_c	Coating breakdown factor	-
I	Current requirement	A
I_m	Mean current demand	A
I_{out}	Anode current output	A
i	Current density	A/m^2

i_0	Exchange current density	A/m^2
$i_{0,a}$	i_0 at anode	A/m^2
$i_{0,c}$	i_0 at cathode	A/m^2
i_{av}	Average current density	A/m^2
i_{corr}	Corrosion current density	A/m^2
i_{mud}	PC slope in mud	$\frac{A}{m^2V}$
i_{sea}	PC slope in seawater	$\frac{A}{m^2V}$
J	Total number of stress range bins	-
k	Scaling factor	-
M_{anode}	Total anode mass	kg
m	Material parameter	$\frac{mm}{MPa(mm^{0.5})^m}$
m_{FC}	Negative SN-curve Slope for FC	$\frac{mm}{MPa(mm^{0.5})^m}$
m_{CP}	Negative SN-curve Slope for CP	$\frac{mm}{MPa(mm^{0.5})^m}$
N	Number of cycles	-
N_j	Number of cycles to failure at a constant stress range ΔS_j	-
n	Ion charge	$\frac{mol}{mol}$
n_j	Number of cycles accumulated at stress S_j	-
Q	Anode capacity	Ah/m
R	Natural gas constant	$\frac{J}{mol\,K}$
R_{anode}	Anode resistance	Ω
r_0	Initial anode radius	mm
r_{final}	Final anode radius	mm
T	Absolute temperature	K
T_{MP}	Design lifetime MP	$years$
T_{CP}	Design lifetime CP system	$years$
t	Time	$years$
t_0	Normalized initial time	-
t_{av}	Normalized time for average conditions	-
u	Utilization factor	-
V_{corr}	Maximum corrosion rate	$mm/year$
x	*Numeration*	-

Greek Symbols	Description	Unit
α	Charge transfer coefficient	-
ΔS_j	Stresses ranges	MPa
ΔV	Potential difference/driving voltage	V
ϵ	Anode capacity	Ah/kg
η	Overpotential	V
ρ	Density	kg/m^3
σ_{sea}	Seawater conductivity	S/m
σ_{mud}	Mud conductivity	S/m

Chemical Symbols	Name
Al	Aluminum
Ag	Silver
Cl	Chlorine
Cu	Copper
Fe	Iron
H	Hydrogen
Mg	Magnesium
$AlCl_3$	Aluminum chloride
$CaCO_3$	Calcium carbonates
H^+	Hydron
H_2O	Hydrogen oxide, water
O_2	Oxygen
OH	Hydroxide
$Fe(OH)_2$	Ferrous hydroxide
$_4Fe(OH)_3$	*Rust*
$Ag/AgCl^-$	Silver/Silver-Chloride
$Cu/CuSO_4$	Copper/Copper-Sulfate

1 Introduction

Offshore wind became a promising approach as a renewable energy resource during the last decades. Since the first offshore wind farms (OWFs) face the end of their service life in the upcoming years, lifetime extension of offshore wind turbines (OWTs) becomes increasingly relevant for research and industrial implementation. Prolonged operation time would save on investment and planning cost of new wind farms. Furthermore, it would lead to increasing revenue of existing OWFs. To ensure a safe and economic operation after design life, assessment of all wind turbine components is required. Structural integrity is one of the main factors to decide whether lifetime extension is feasible [1].

1.1 Problem Statement

Offshore structures are mostly located in harsh environments threatened by wind and wave loads. Parts of the steel foundations are permanently or frequently exposed to salty water and hence, marine structures are subject to corrosive and biological stresses. Environmental conditions like humidity, duration of wetness, chlorides, temperature, and sunlight abet corrosion [2]. For offshore foundations main governing parameters, like seawater temperature, concentration of dissolved oxygen, sea current, marine growth and calcareous deposit layers, as well as salinity are crucial to corrosion [3].

In opposition to oil and gas structures, which are also located in offshore conditions, a wind turbine is exposed to high dynamic loads leading to risk of fatigue damages [4]. Corrosion and fatigue loads are crucial problems threatening the structural strength of OWTs and are responsible for degradation and failures [5].
Corrosion reduces the fatigue resistance of a structure which is shown in the recommended practice of *Det Norske Veritas and Germanischer Llyod* (DNV GL) RP-C203 [6]. For a given structure subjected to high fatigue loads the number of load cycles until failure, e.g. the service life, is typically 3 to 5 times higher in case of corrosion protected compared to free corroding [6, 7]. Therefore, corrosion control systems are essential to not only predict and prevent failures in an early stage but also to save on costs. Contribution of a corrosion protection systems plays a decisive role for quantitative estimations on monopile (MP) lifetime, which is either treated under free corrosion (FC) or under protection. If it comes to MP lifetime extension (LTE), the question whether a corrosion protection system is still performing

becomes highly significant.
Mounted cathodic corrosion protection systems for offshore applications are usually difficult to estimate and accompany with cost-intensive maintenance and risks; mass and size inspection are nearly unfeasible.

At last, corrosion and its control is a very complex, time-dependent process afflicted with high uncertainties and becomes increasingly crucial for OWFs aiming LTE.

1.2 Literature Review

While research on lifetime extension is increasing in wind industries, publications on experiences with corrosion and its protection in the offshore wind energy industry are limited. Luengo et al. worked on failure mode identification for end of life scenarios of OWTs [8]. Focus on fatigue failure assessments for lifetime extension of offshore substructures is researched by Ziegler et al. [9–11].
Several researchers like Momber, Hempel and Heins et al., and others worked on corrosion control and protection for offshore wind energy devices; types of corrosion and practical solutions to prevent corrosion are discussed in their papers [12–17]. In February 2017, a review on the current status and future perspectives of corrosion protection systems in offshore wind structures was published by Price and Figueira [5]. However, this study mainly points out the application of coatings for OWTs. The application of cathodic protection (CP) with focus on polarization of metals in offshore environments is analyzed in detail by Hartt et al. [18–22].
References from oil and gas as well as ship industry provide a fundamental understanding on corrosion in marine environments and the protection possibilities. DNV GL published first design assumptions for corrosion protection systems for OWTs in the recommended practice (RP) 'Corrosion Protection for Offshore Wind Turbines' in 2016 [23]. In an earlier RP from DNV (RP-B401 [3]) a guideline for traditional Cathodic Protection Designs is suggested based on anode mass and current calculations. The *Federal Maritime and Hydrographic Agency* (BSH) and the *Federal Waterways Engineering and Research Institute* (BAW) are working on standards for requirements of corrosion protection in the sector of offshore structures and components [24–26].
NACE International is a worldwide corrosion authority and published standards for corrosion control and measurement techniques for offshore structures [27, 28]. ASTM International is providing standard practices to calculate corrosion rates [29].

To the knowledge of the author there are no studies published considering cathodic corrosion protection for offshore wind structures to predict on lifetime by calibrating simulations with on-site measurements.

1.3 Research Objective and Targets

The problem statement and review of literature lead to the question:

Is there a possibility for prolonged service life of cathodic protection systems for further estimations on lifetime extension of monopile-based offshore wind turbines?

The main target of this thesis is to evaluate service life of cathodic corrosion protection systems to further decide whether LTE for OWTs is feasible. Corrosion protection is mainly given by CP and coating. However, in this thesis only CP is investigated.

Data from on-site measurements will be compared with design values and applied to calibrate cathodic corrosion protection simulations. The practical implementation is critically questioned considering model uncertainties but also uncertainties following from on-site measurements. Sensitivity studies address the robustness and representativeness of results.
Cost-efficient solutions for maintaining corrosion protection become important for the relevance of LTE of an OWT. Sufficiently informative model outcomes, providing additional information on corrosion behavior and protection progress, could save on costs from on-site measurement and operations.

The approach is performed by means of COMSOL Multiphysics®, a finite element method based software and the computing environment MATLAB®. On-site measurement data is provided from wind farms located in the North Sea and confidentially treated. Loads are available from a research turbine (*National Renewable Energy Laboratory*) based on a MP foundation from the *OC3 Project* and further processed by Ziegler [30].

1.4 Outline of the Report

The study is based on simulations and results are documented in this report, sectioned in the following chapters:

- In **Chapter 2** an overview is provided containing 'State-of-the-Art' and theoretical backgrounds of the chemical corrosion process. A brief introduction explains the corrosion process especially in seawater. Corrosion protection with a focus on cathodic corrosion protection for offshore MP is illustrated. Additionally, the modeling software COMSOL Multiphysics® is summarized.

- **Chapter 3** illustrates the applied methodology to estimate on corrosion protection lifetime by combination of measurement data and simulation. Data is used to calibrate corrosion kinetics and analyze CP lifetime. Furthermore the implementation for LTE of monopile-based OWTs is elucidated.

- In **Chapter 4** results on cathodic corrosion protection lifetimes are presented and critically discussed considering their sensitivity and robustness. A case study shows how lifetime of CP systems influences service life of a MP. Limitations for practical implementations are mentioned, concluded with economical and environmental aspects.

- Conclusion and recommendations for future works are closing the thesis in **Chapter 5**.

- Additional plots and illustrations are attached in the **Appendix**.

2

Theoretical background and State-of-the-Art

Metallic materials in aqueous and gaseous environments are exposed to corrosive attacks. Corrosion is a natural process of material degradation controlled by thermodynamic and kinetic expressions. The corrosion rate is stated as thickness loss per year [mm/year]. In order to implement a fully working corrosion protection system, knowledge on its kinetic expression must be available. The next sections describe thermodynamic and kinetic fundamentals with a focus on corrosion of metal in saltwater (seawater) and possibilities to reduce the corrosion rate by corrosion control.

2.1 Thermodynamics of Corrosions

Thermodynamics of corrosion are describing the relation between chemical and electrical energy when a metallic material comes in contact with an electrolyte. This electrochemical process consists of two partial reactions, so called half-cell reactions or half-reactions. The anodic reaction is an oxidation reaction and explains the dissolution of a metal in an electrolyte, e.g. salty water. The anodic dissolution at the metal surface is given by the following equation [31]:

$$2\,\mathrm{Fe} \longrightarrow 2\,\mathrm{Fe}^{2+} + 4\,\mathrm{e}^{-} \tag{2.1}$$

The metal disposition mentioned in the anodic half-cell reaction in Equation 2.1 is completed by a reduction reaction (cathodic reaction) occurring on the same electrode reducing oxygen and pH value. In acidic solutions the oxygen reduction reaction is:

$$\mathrm{O}_2 + 4\,\mathrm{H}^{+} + 4\,\mathrm{e}^{-} \longrightarrow 2\,\mathrm{H}_2\mathrm{O} \tag{2.2}$$

The half-cell oxygen reduction reaction in alkaline or neutral solutions containing O_2 according to Roberge is [31]:

$$\mathrm{O}_2 + 2\,\mathrm{H}_2\mathrm{O} + 4\,\mathrm{e}^{-} \longrightarrow 4\,\mathrm{OH}^{-} \tag{2.3}$$

The reaction product OH^{-} rises the pH level. Higher pH levels lead to a more alkaline solution.
The complete reaction in an electrolyte from anode to cathode is the sum of both half-cell reactions, shown in the following equation [31]:

$$2\,\mathrm{Fe} + \mathrm{O}_2 + 2\,\mathrm{H}_2\mathrm{O} \longrightarrow 2\,\mathrm{Fe(OH)}_2 \tag{2.4}$$

The reduction of oxygen on the cathodic side is explained by an electron transfer across the interfaces (electrons are received from the base metal), whereas the anodic reaction of dissolved metals transfers electrons (electrons are sent into the base metal). The resulting product ferrous hydroxide ($Fe(OH)_2$) is a pre-product of rust. An additional reaction with dissolved oxygen converts $Fe(OH)_2$ in hydrous ferric oxide $_4Fe(OH)_3$, which is commonly known as rust [31].

Driven by the free energy change of the partial reactions a transfer process takes place at the interface between metal surface and electrolyte. This driving force is also called the electrode potential. The Nernst-Equation explains the relation between the electrode potential at the reduction reaction E_{red} and the equilibrium or half-cell potential E_{eq} [32, 33]. At E_{eq} each half-cell reaction is under its steady-state condition.

$$E_{red} - E_{eq} = \frac{RT}{nF} \, ln \left(\frac{a_{ox}}{a_{red}} \right) \tag{2.5}$$

where:
a_{ox} = chemical activity for oxidation
a_{red} = chemical activity for reduction
R = natural gas constant ($8.314 \, \frac{J}{mol\,K}$)
T = absolute temperature at standard conditions (278 K)
F = Faraday constant ($96{,}487 \, \frac{As}{mol}$)
n = ion charge $[\frac{mol}{mol}]$

2.2 Kinetics of Corrosion

Kinetics of corrosion describe how fast the corrosion proceeds and can be explained by the mixed-potential theory. This theory includes differing anodic and cathodic polarization occurring at the same time and can be used to examine on corrosion behavior and control of corrosion rate [31–35].
When a metal is submerged in an electrolyte, cathodic and anodic reactions happen simultaneously driven by a natural electrode potential. An electron transfer through the metal surface proceed until the equilibrium potential is reached. The steady-state potential, also called corrosion potential E_{corr} usually differs from the electrode potentials, but is the balance somewhere in between the potential of the anodic (metal dissolution) and cathodic (oxygen reduction) reaction. It is dependent on the rate of cathodic and anodic reactions. The charge transfer between the two interfaces is explained by a kinetic expression. It is limited by the current density i, which is the current in ampere [A] that flows through a surface per square meter [A/m^2].
The difference between a potential E and the corrosion potential E_{corr} is the over-potential η in Volt [V], described in the following equation [35]:

$$\eta = E - E_{corr} \tag{2.6}$$

The overpotential is zero when both, the anodic and cathodic current flow are equal, but in opposite directions (net current flow equals zero). It should be noted here, that the current flow at the cathodic side is notated as a negative flow. The over-potential is depending on the current density i, since i induces a change in the electrode potential due to ohmic losses. Those losses are related to the resistivity of the electrolyte, the contact resistance between the leads, and possible deposit layers on the surfaces [35].

The relation of overpotential and current density can be illustrated by polarization curves (PCs), where η is plotted over i or rather in a logarithmic scale $log(i)$. An Evans Diagram is a simplified graphical representation of the mixed-potential theory to show anodic and cathodic polarization behaviors (c.f. Figure 2.1). The negative cathodic current is plotted positively to illustrate the corrosion potential E_{corr} as an intersection point. This point shows the corrosion current density i_{corr} on the x-axis.

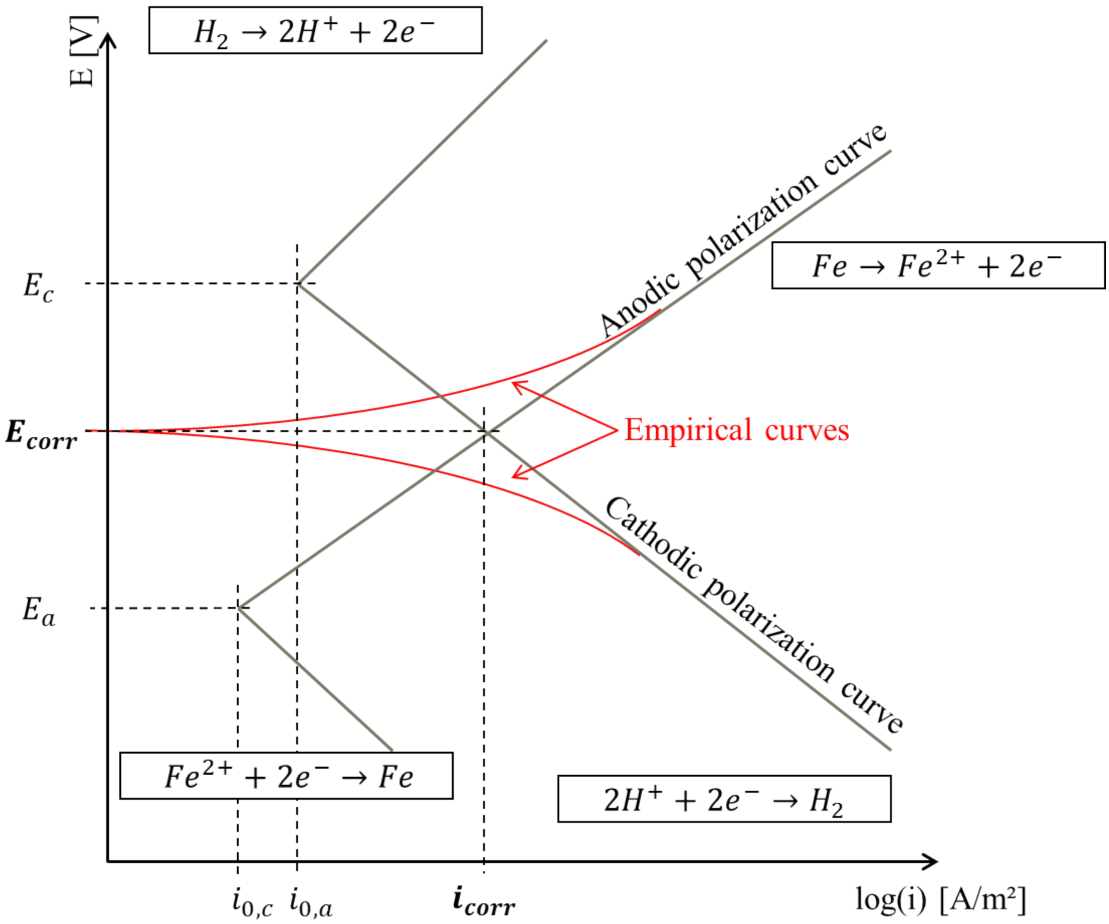

Figure 2.1: Schematic Evans Diagram

In Figure 2.1 it is seen that the anodic (loss of electrons) and the cathodic curve (gain of electrons) intersect at the corrosion potential E_{corr}, where i_{corr} is at its maximum. This value is used to calculate the corrosion rate by means of kinetic expressions. E_a and E_c are the natural anodic and cathodic potentials, $i_{0,a}$ and $i_{0,c}$

the related exchange current densities.
The Tafel equation, as a kinetic expression, describes the overpotential based on the Butler-Volmer theory. This fundamental formula explains a polarization of an electrode, which means in detail the accurate relation between electrode current density i, the exchange current density i_0, and overpotential η when both, anodic and cathodic reactions occur at the same electrode. The Butler-Volmer process is reversible [31, 32].

$$i = i_0 e^{\frac{\alpha n F \eta}{RT}} - i_0 e^{\frac{-(1-\alpha) n F \eta}{RT}} \tag{2.7}$$

where:
i_0 = empirical value for initial current density $[\frac{A}{m^2}]$
η = overpotential [V]
α = charge transfer coefficient (between 0 and 1)
n = ion charge $[\frac{mol}{mol}]$
F = Faraday constant (96,487 $\frac{As}{mol}$)
R = natural gas constant $[\frac{J}{molK}]$
T = absolute temperature at standard conditions (278 K)

For overpotentials larger than 50 mV (and small i_0 values) Equation 2.7 can be simplified to an irreversible process:

$$i = i_0 e^{\frac{\alpha n F \eta}{RT}} \tag{2.8}$$

The overpotential results by rearranging Equation 2.8 to the irreversible Tafel equation. The overpotential η_c for cathodic reactions is then:

$$\eta_c = A_c log(\frac{|i|}{i_0}) \tag{2.9}$$

where:
i = current density $[\frac{A}{m^2}]$
i_0 = initial current density $[\frac{A}{m^2}]$
A_c = cathodic Tafel slope [V]

A_c equals the fraction $RT/\alpha nF$; i_0 is zero when overpotential is zero.
A typical value for A_c according to Stern [35] is -0.1 V. This corresponds to a exchange current density of $i_0 = 0.001\,A/m^2$. The Tafel equation is often applied for theoretical evaluation of hydrogen induced corrosion phenomena. The corrosion process of metal in seawater can also be assumed as linear according to expert opinions.

2.3 Corrosion in Seawater

When a metal is in contact with a sodium chloride (NaCl) solution containing oxygen (O) aqueous corrosion occurs, driven by the specific electric potential between the metal and the seawater. Seawater is a solution of oxygen, hydrogen (H_2O), and dissolved salts, like NaCl. Other components of seawater are: magnesium, vanadium, sulfur, calcium, potassium, bromide, and carbon. The salinity is usually between 3.1% and 3.8% [3]. The pH value of seawater is around 7.5 to 8.4 and can decrease due to acidification or increase with higher hydroxide (OH^-) production [32, 36, 37].

The electrical conductivity of seawater σ_{sea} varies between 2.0 and 5.0 S/m in the North Sea, but can be higher or lower in other spheres. Seawater conductivity or its inverse, resistivity, is highly dependent on temperature and salinity (NaCl content). As higher the salinity and temperature, as higher the conductivity [3]. In the theoretical case of zero resistance the current could flow infinitely far.

According to DNV temperature, salinity, oxygen content, seawater velocity, water current, water depth, marine growth, and the chemical composition of water are affecting corrosion and its protection [3]. All environmental parameters can vary with geographical location and season.

2.4 LTE of Offshore Structures (Monopiles)

The fatigue lifetime of a structure is limited by the most critical spot, where the first failure is expected to occur. This hotspot must be individually evaluated for each case.
To allow for LTE of an OWT remaining useful lifetime (RUL) must be certified based on a 'current state-of-the-art assessment' of all wind turbine components, as stated in DNV GL's standard ST-0262 for 'Lifetime extension of wind turbines' [1].

If service life of an offshore structure (here: MP) is threatened by fatigue damages SN-curves are applied. This approach evaluates the possible bearable number of cycles N (as a representation of fatigue life) for a specific stress range ΔS until a material failure occurs. SN-curves are empirically established by material tests. The characteristic of a SN-curve is given in the following equation [7]:

$$log(N) = log(a) - m\, log\left(\Delta S\left(\frac{d}{d_{ref}}\right)^k\right) \tag{2.10}$$

N = number of cycles
$log(a)$ = intercept of the x-axis
m = material parameter $\left[\frac{mm}{MPa(mm^{0.5})^m}\right]$
ΔS = stress range $[MPa]$
d = wall thicknesses (of MP) $[mm]$
d_{ref} = reference thickness $[mm]$
k = empirically determined scale value [-], recommended by DNV GL OS-J101 [7]

The material parameter m is the negative slope of the SN-curve in a double logarithmic scale. For a welded section under FC a m_{FC} of 3 is assumed according to

DNV GL RP-C203 and OS-J101 [6, 7], whereas the slope flattens for corrosion protected surfaces with $m_{CP} = 5$, after a specified number of cycles (here: $N = 10^6$).

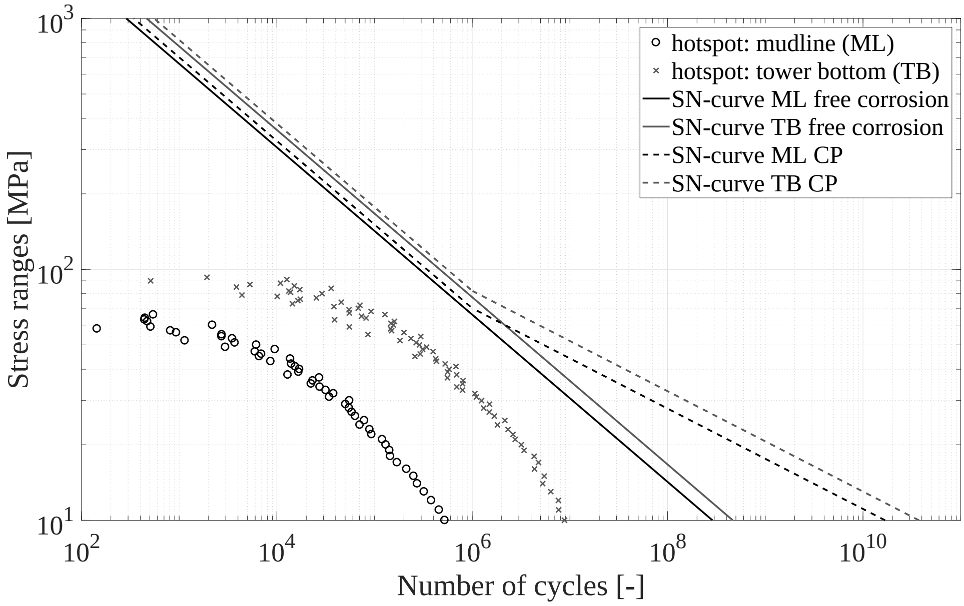

Figure 2.2: Exemplary SN-curve for loads over 20 years according to Ziegler [30]

Figure 2.2 shows that the case of FC the MP material is less durable compared to MP material protected by CP.
The lifetime is directly linked to the number of cycles N, which is shown by Miner's rule [7]:

$$D = \sum_{j=1}^{J} \frac{n_j}{N_j} \tag{2.11}$$

where:
D = fatigue damage value (for D=1: failure occurs)
J = total number of stress range bins
n_j = number of cycles accumulated at stress S_j
N_j = number of cycles to failure at a constant stress range ΔS_j

Damage values for materials exposed to FC are higher compared to D-values for cathodic protected materials.

Corrosion protection externally is usually designed for the whole lifetime of a structure; service lives of internal CP systems are often shorter than MP design lifetime, since depleted anodes can be replaced when needed. Lifetime of a MP is calculated by means of damage values for CP during the service life of the CP system. When anodes are completely consumed or CP fails due to any other reason, lifetime of MPs must be reevaluated by means of the FC damage value D_{FC}.

2.5 Corrosion Protection for Offshore Foundations

Offshore corrosion control implies corrosion protection, corrosion allowance (CA), and the usage of corrosive resistant materials. Corrosion protection techniques can be generally divided in active and passive systems. In the context of this study the latter includes coatings, which shield the structure from aggressive environments (e.g. seawater). The method of active corrosion protection, also known as cathodic corrosion protection, makes the surface, that should be protected, to the cathode by implementing anodes of less noble materials or by inert anodes subjected to impressed current.

An OWT consists of a foundation, the transition piece (TP), the tower, and the turbine (nacelle, rotor) itself. Foundations are build as different constructions, like MPs, tripods, jackets, or floating systems. Their application is depending on several factors, e.g. water depth and turbine size. MPs are usually conical steel (S235ML) pipes with external lower diameters approximately around 4 to 9 m, upper diameters are usually some meters smaller. The wall thickness of a MP with a diameter of 5 to 6 m is around 50 to 90 mm at mudline and can become 10 to 50% slimmer up to the MP tip (tower bottom (TB)). The MP length can vary between 20 m and 90 m, depending on water depth and soil conditions. The lower part of the MP is rammed into the seabed. Depending on soil type the buried part can be more than half of the MP length. The TP is connected to the foundation by a flange and bolts, which create an electrical connection between TP and MP. If the electrical contact ensured by the flange-bolt connection fails, dedicated cables are installed to ensure good electrical contact.
The parts listed above are summarized in the category 'primary steel'. Failures at primary steel parts have a major significance for the lifetime of the whole WTG. Whereas the consequences of failures in 'secondary steel' parts including boat landing, ladders, platforms, etc. might be minor.

For the application of corrosion control for an offshore monopile-based wind turbine the structure is divided in different zones according to DNV GL [23] as shown in Figure 2.3. Figure 2.4 explains the notification of different water levels.

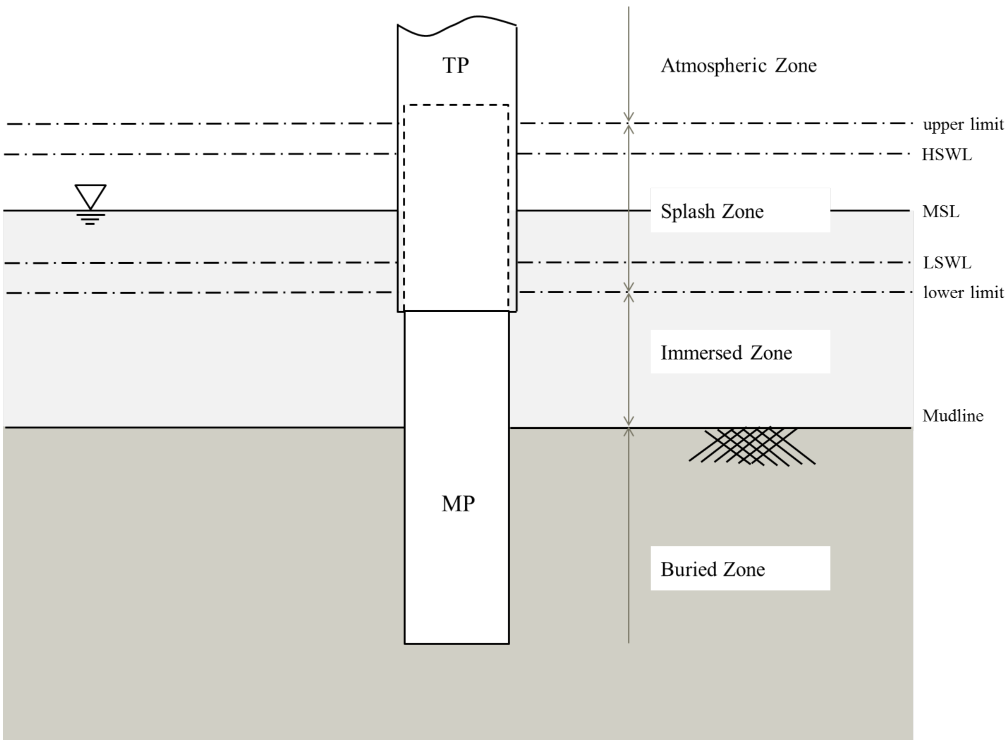

Figure 2.3: Schematic zones an OWTs can be divided in according to DNV GL RP-0416 [23]

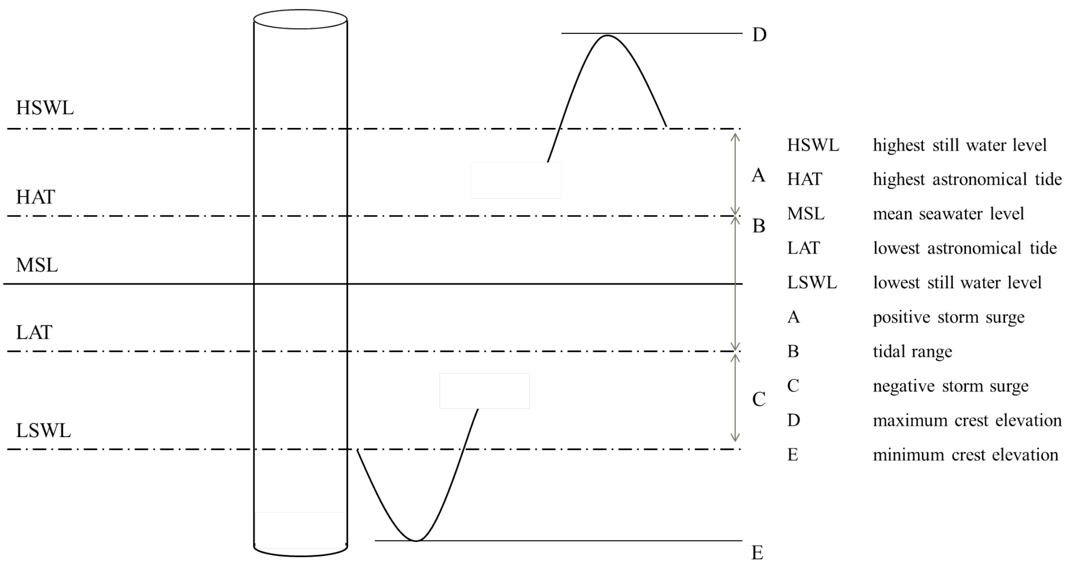

Figure 2.4: Schematic seawater levels according to IEC 61400-3

Atmospheric Zone is mainly exposed to sunlight, wind, and external weather conditions. According to RP0416 [23] the atmospheric zone shall be coated.

According to DNV GL's RP-0416 [23], the *Splash Zone* is intermittently in contact with water and air due to tidal movement and wave action. The upper limit is the high still water level (HSWL) plus the 'crest height of a reference wave whose height is equal to the significant wave height with a return period of 1 year' [23], consequently the lower level is the low still water level (LSWL) minus 'crest height of a reference wave whose height is equal to the significant wave height with a return period of 1 year' [23]. Coating is mandatory for all external parts of primary steel from 1 m below mean seawater level (MSL) upwards with an additional allowance for FC. Internally either CA or coating can be applied. CP systems are mandatory externally and suggested internally in the lower part of the splash zone (below MSL). It should be ensured, that anodes are always submerged. Corrosion protection for secondary steel shall be assessed based on risks to the environment and humans as well as maintenance and repair possibilities [23].

The *Immersed Zone* begins below the lower limit of the splash zone and is permanently exposed to seawater. This region shall be protected internally and externally by CP systems which can be supported by coating [23]. It should be noted here, that an increasing focus is set on consideration of scour and microbial corrosion (MIC) around the MP near the seabed. Internally either CP or allowance for FC with or without coating is suggested.

The part below mudline buried in soil is the *Buried Zone*. Usually corrosion protection is only applied for a small part of the MP in soil (first meters below mudline), therefore the current requirement must be given by the corrosion protection system mounted above mudline. However, soil drains current from the CP systems and must therefore be considered when designing a protection system [23]. Scour reduces the buried area, whereas soil push-up lifts the mudline and with that increases surface area in soil.

According to RP-0416 published by DNV GL [23], CA, in the case of FC on several structural parts, corresponds to:

$$CA = V_{corr} \cdot (T_{MP} - T_{CP}) \tag{2.12}$$

V_{corr} = maximum corrosion rate $[\frac{mm}{year}]$
T_{MP} = design lifetime of the structure (here: MP) $[years]$
T_{CP} = design life of the corrosion protection $[years]$

T_{CP} equals zero in case of no corrosion protection. FC is either expected from the beginning (if designed so) or occurs after the corrosion protection system reaches its lifetime.

2.6 Coating

Coating is a passive corrosion protection, which shields the steel surface from seawater and harsh environmental conditions. Coating specifications are defined in several standards from NACE, NORSOK M-501 [38], or ISO 12944 [39] and ISO 20340 [40]. Coated parts should be frequently inspected for fatigue cracks in the coat. The usage in immersed parts is less recommended as a sole protection solution, since inspections are cost-intensive. However, if coating is applied underwater, it supports the CP system by reducing the current requirement on the MP surface. Current requirement is approaching zero for fully electrically insulated coatings (100% insulating). Mechanical damages and aging lowers the electrical insulation capacity of the coating. This anticipated coating deterioration can be defined by the coating breakdown factor f_c. In case of $f_c = 1$ the coating has no current reduction effect. According to DNV GL f_c can be expressed by a linear function over time t in years [3]:

$$f_c = a + b \cdot t \tag{2.13}$$

a and b are constants defined by codes or individually determined, depending on coating category and environmental conditions.

2.7 Influence of Calcareous Deposit

An indirect influence on current requirements (and the PC) for a CP system in seawater has calcareous deposit. Calcium carbonates ($CaCO_3$) and hydroxides (OH^-) form a shielding layer on the metal surface, which reduces oxygen access to the surface and thereby reduces current requirements for CP.
Aluminum Chlorides $AlCl_3$(s), resulting from dissolving Aluminum anodes in salt water, lower the pH value nearby the anodes and lead to a more acidic environment. This effect ensues a reduced discharge of hydrogen ions, whereby H^+ activity is also decreased [41]. Acids, in general, dissolve chalky substances. Hence, the calcareous deposit layer is strongly influenced by the pH value of the electrolyte. Low pH values (acidic solution) increase the corrosion rate; for high pH values (alkaline or base solutions) the corrosion rate is reduced [42, 43].

Formation of calcareous deposit is also depending on weather seasonality [3, 42, 44]. During summer periods a formation of calcareous layer on the MP surface is favored, which is a consequence of the higher water temperature (in the North Sea around 10 to 15 °C) and with that of higher seawater conductivity and current densities. Additionally, marine growths can be built on parts of the MP surface in summers. In colder periods calcareous deposit shrinks in area and thickness, mainly due to a reduced seawater conductivity [45]. Marine growths recede when temperatures drop down. Storm events can also be responsible for reduction in calcareous layer and marine growths [3].

2.8 Cathodic Corrosion Protection Systems

According to ISO 8044 cathodic corrosion protection is the 'electrochemical protection by decreasing the corrosion potential to a level at which the corrosion rate of the metal is significantly reduced' [46]. In this electrical cell the protected surface is the cathode [28].

In an active corrosion protection systems anodes act as a current source for the CP system. Electrons produced from the anodes flow to the cathode to prevent the metal dissolution, explained in Equation 2.1. The kinetic expression between the electrolyte (seawater) and the metal surface is controlled by cathodic polarization. The schema of a CP system is shown in Figure 2.5.

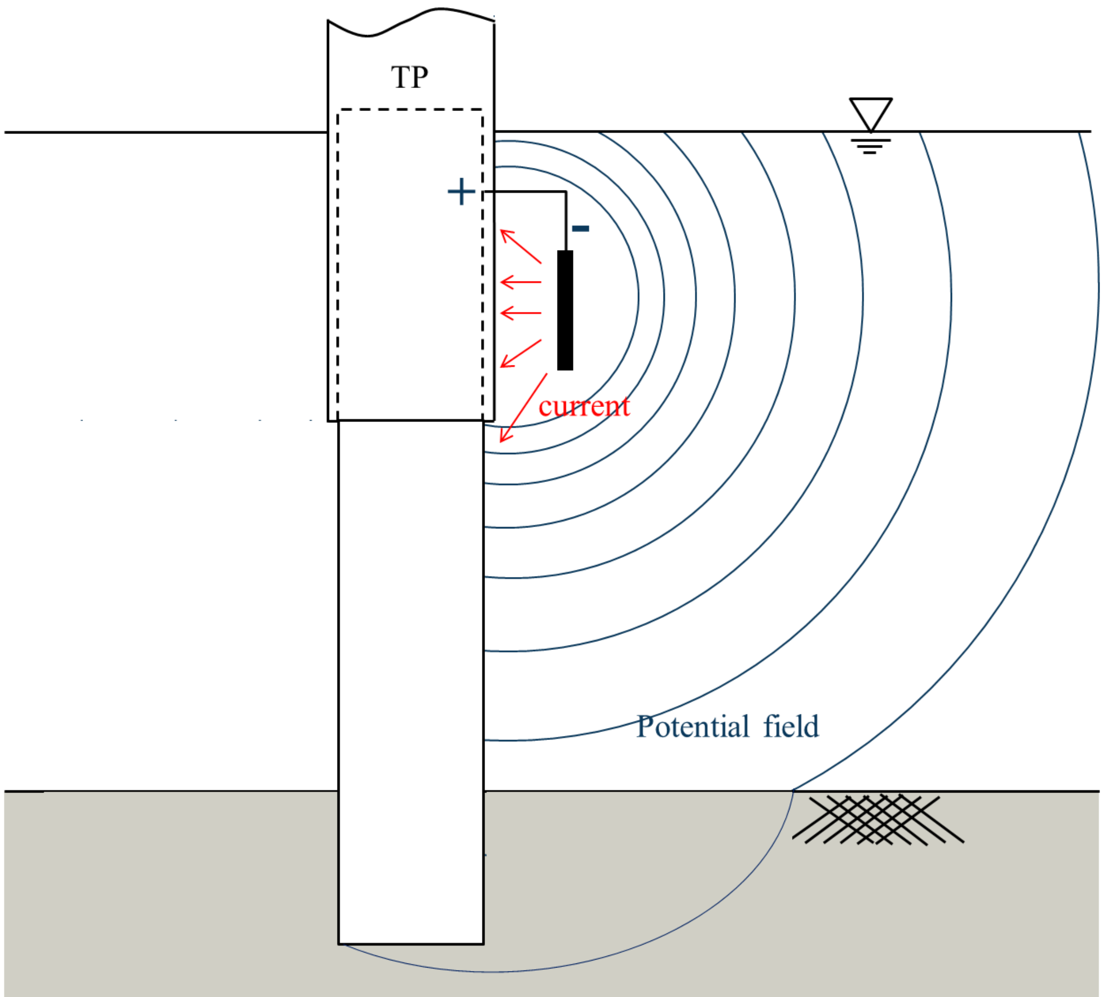

Figure 2.5: Schematic CP system of an offshore MP by an anode sending out current (red arrows) and generating a potential field (blue lines).

Potential field lines and current flow originated from the anode are illustrated qualitatively in Figure 2.5. Potential expansion in soil differs from potential spread in

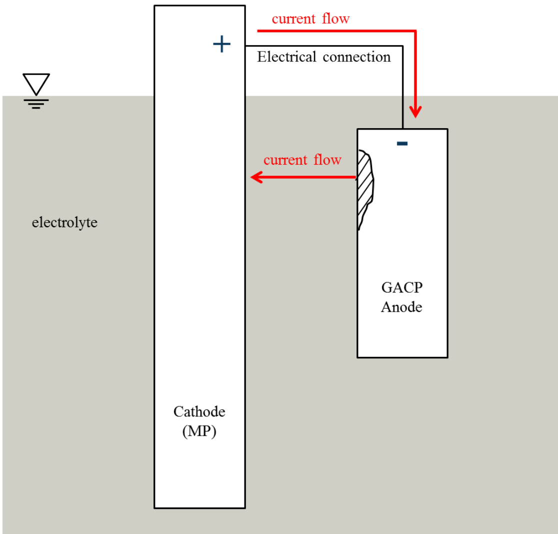

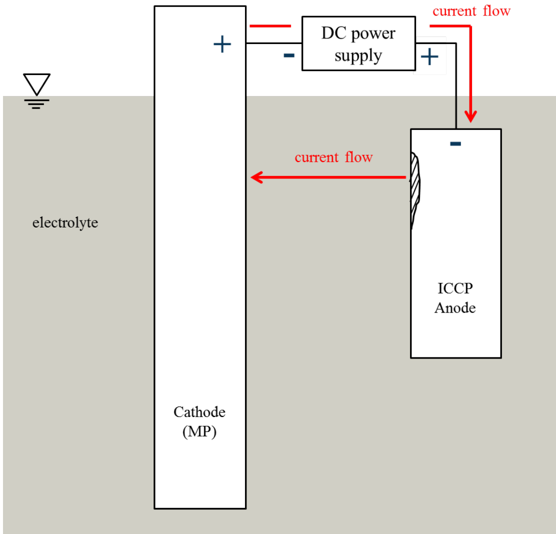

Figure 2.6: Schematic GACP principle **Figure 2.7:** Schematic ICCP principle

seawater due to a higher soil resistivity. CP systems can be either a galvanic anode cathodic protection (GACP) as seen in Figure 2.6 or an impressed current cathodic protection (ICCP) illustrated in Figure 2.7. Decisions on systems applications are made individually by wind farm owners and operators. In both cases, anodes can be mounted horizontally or vertically on cages either at the TP or at the MP, but usually above sediment.

2.8.1 GACP

A GACP system is equipped with so called 'sacrificial anodes', which are consumed while protecting the cathode from corrosive dissolution. Therefore, one prerequirement for GACP systems is that the anode material is less noble than the structure material. Alkaline metals like aluminum (Al), magnesium (Mg), or zinc (Zn) are possible materials, whereas aluminum alloys are most commonly applied offshore. Anode specifications are mentioned in several standards from DNV [3] or by anode manufacturers.

Anode Design and Installation

To successfully avoid corrosion the anodes must be able to provide the required amount of electrical current faster at the cathode than the oxygen in seawater reacts with the metal. The required current density at the cathodic side i_c is dependent on several location-specific environmental parameters. The dependency on water temperature is a strong indicator for variations in current density over winter and summer periods. Marine growth and calcareous deposit, which both form in warmer months, might also have an influence on current requirement, as stated in Section 2.7. Recommended values for i_c are documented in standards, e.g. RP-B401 [3] from DNV. Values are divided in different stages: initial, mean, and final. The initial phase indicates a very high anode current output. It is expected that a calcareous

deposit layer is formed within the first weeks in which the corrosion protection systems is operating. Theoretically calcareous layer keeps on forming over the whole service time of the CP system and could be illustrated by a negative exponential curve.
The initial current requirement decreases continuously until it reaches a stabilized value (mean value). In case of a storm event the calcareous deposit and marine growths can break down. Furthermore, too high acidification of the seawater dissolves the calcareous deposit layer. Both aspects imply a slight increase in current density requirement, from the mean value to the final current density value.

DNV recommends a simplified analytical approach in RP-B401 [3] to evaluate the anode mass required for protection of the whole structure over a specified lifetime. Primary this code was developed for jackets, where the anodes are equally distributed around the whole structures. Whereas the anodes at a monopile-based structure are usually grouped in cages at the TP or MP due to elderly design issues, but are not evenly spread over the whole submerged part. The traditional method - introduced in the following steps - should therefore be regarded with caution, when it comes to lifetime predictions of CP systems for monopile-based OWTs:

Step 1: Current requirement I in ampere [A]

$$I = i_c \cdot A \cdot f_c \tag{2.14}$$

where:
i_c = required current density $[\frac{A}{m^2}]$ according to DNV [3]
A = surface to be protected $[m^2]$
f_c = coating breakdown factor [-] according to coating suppliers

For bare-steel surfaces the coating breakdown factor is 1.

Step 2: Required total anode mass M_{anode}

$$M_{anode} = \frac{I_m \cdot T_{CP} \cdot 8760}{u \cdot \epsilon} \tag{2.15}$$

where:
I_m = mean current demand $[A]$
T_{CP} = design lifetime $[years]$
u = utilization factor [-]
ϵ = electrochemical capacity of anode material $[\frac{Ah}{kg}]$

8760 are the number of hours per year. u is usually 0.9, given by anode manufacturers; Minimum capacity is 2500 Ah/kg for aluminum anodes and 780 Ah/kg for zinc anodes [3].

Step 3: Protection potential ΔV and maximum anode current output I_{out}

$$I_{out} = \frac{\Delta V}{R_{anode}} \tag{2.16}$$

where:
ΔV = potential difference/driving voltage $[V]$
R_{anode} = anode resistance $[\Omega]$

The anode resistance R_{anode} is specific for each anode shape and type. Formulas to estimate R_{anode} are provided in standards, e.g. RP-B401 [3], or manufacturer specification.

Step 4: Assumed consumption of anode mass

$$C = M_{anode} \cdot \epsilon \cdot u \tag{2.17}$$

where:
C = anode current capacity $[Ah]$
M_{anode} = total anode mass $[kg]$

Finally it is tested that the number of anodes (x) times the capacity is greater or equal to current output I_{out} for the specified time (here: T_{CP}):

$$x \cdot C \geq I_{out} \cdot T_{CP} \cdot 8760\,[h/year] \tag{2.18}$$

where x is the number of anodes.

The calculated number of anodes (considering the calculated total mass M_{anode}) should be arranged in a practicable way, that protection is as equally distributed as feasible over the whole submerged part of the MP. A minimum distance from the anodes to the MP surface should be adhered. The anodes located at the MP surface send out current and with that they create a potential field (c.f. Figure 2.5). These potential lines become less negative as further they are away from the anodes. Care should be taken in order to avoid anode interference effects and principally also for overprotection [3]. The former can occur when anodes are located too close to each other reciprocally interfering their current output and with that the total current, which can reach the MP surface, might be reduced. Overprotection can lead to embrittlement of the metal surface and would occur for potentials more negative than $-1.15\,\mathrm{V}$. However, overprotection is eliminated by less negative anode potentials when using the normal GACP anode materials: aluminum (E_{Al} = -1.0 to $-1.1\,\mathrm{V}$ [3]) and zinc (E_{Zn} = -0.95 to $-1.05\,\mathrm{V}$ [3]).

2.8.2 ICCP

The ICCP system, as a long-term protection method, uses a rectifier to supply the required current. ICCP systems are also based on the active corrosion protection method, but need an external DC power supply to provide the protection potential. The power supplier (also called rectifier) is connected to both, the anodes and the steel surface. The negative pole of the rectifier is connected to the steel structure (cathode), whereas the positive output is connected to the anode. Electrons supplied from the rectifier are sent to the surface and thereby prevent the disbandment of the metal [12, 14]. The ICCP anode material is slightly soluble into metallic ions, like

graphite or platinum. Since electrons are provided mainly by DC power supply, the decomposition of the anode itself is very slow [23]. According to DNV GL at least two permanent reference electrodes must be implemented for offshore applications to continuously measure the potential difference ΔV, mainly to prevent overprotection [23]. By means of the DC power supply the current or the voltage can be adjusted when potential varies caused by e.g. environmental changes.
Potential measurements from reference electrodes as well as anode current output and DC voltage are monitored, usually in 10-minute time steps. Additionally, the ICCP system can be equipped with an alarm to alert in case of overprotection. Anode interference can occur as explained in Section 2.8.1 and should be avoided when designing an ICCP system.

2.8.3 Reference Electrodes

A reference electrode is applied to measure the electrical potential between the metal surface and the reference electrode itself. The potential of steel E_{Fe} is $-0.6\,\mathrm{V}$ [47]. Reference electrodes, practically used for marine applications, are either made out of Silver/Silver-Chloride ($Ag/AgCl^{-}$), Copper/Copper-Sulfate ($Cu/CuSO_4$), or Zinc alloys. The reference value to successfully protect the structure should be more negative than $-0.8\,\mathrm{V}$ ref. to Ag/AgCl/seawater [28], but not more than $-1.15\,\mathrm{V}$ (overprotection). For $Cu/CuSO_4$ electrodes the protection potential is $50\,\mathrm{mV}$ more negative ($-0.85\,\mathrm{V}$). The corrosion protection system must also protect against MIC, if its occurrence is assumed; the protection potential should be more negative ($-0.9\,\mathrm{V}$ ref. to Ag/AgCl/seawater) according to NACE [28].
Manual measurements, performed by offshore personal in periodic time intervals from a platform above water, are required by codes for both, GACP and ICCP systems [23]. For an ICCP system additional reference electrodes are mounted at the structure.

2.9 Corrosion Simulation Software

COMSOL Multiphysics® is a simulation software based on finite element methods to solve physical problems by means of differential equations.

The chemical corrosion model in COMSOL Multiphysics® is a tool to simulate electro-chemical corrosion processes and CP systems. The basic premise of the corrosion model is on current and voltage acting between two electrodes in galvanic cells. This can be applied for several corrosion protection methods, e.g.: anodic, cathodic, or galvanic corrosion. Physics interfaces, like chemical species transports, electro-chemistry, corrosion deformed geometries, porous media, and heat transfer, are used to explain potentials in electrolyte and on electrode structures based on mass and current balance. Reaction kinetics can be described by predefined equations (Tafel, Buttler-Volmer, etc.) or with user-defined functions.
The electro-chemistry interface includes primary, secondary, and tertiary current distribution approaches. The primary current balance on metals is described by

Ohm's law assuming infinitely fast electrode kinetics. The secondary current distribution model is similar to the primary one, but electrode kinetics are finite and account for potential drops. Tertiary distributions are used for non-linear and concentration dependent electrode potential models.
Boundary conditions, like electrolyte behavior, initial values, and electrode characteristics are determined. Reactions are expressed by thermodynamics based on Nernst equation (c.f. Equation 2.5) and kinetics of corrosion.
For all interfaces preset stationary and time-dependent study types are available as well as several meshing options, which are defining the number of nodes. The number of degrees of freedom (DOFs) results from the number of nodes and the number of dependent variables. As higher the number of DOFs, as longer the solution time for one simulation. To solve on electro-chemical models default mesh sizes, triangular (2D) or tetrahedral (3D), are suitable. Mesh size and a so called 'element growth rate' can be selected from predefined settings or individually.
The regarded geometry can be either built directly in COMSOL Multiphysics® or imported as computer-added-design files. A predetermined list offers a wide selection of materials. Additionally, material properties can be set individually if needed.

COMSOL Multiphysics® application library handbooks [48, 49] and model users' guide [50] are providing necessary information on how to module a corrosion controlled problem.

3

Methodology

This chapter describes the methodology to estimate performance time of offshore CP systems internally and externally of a MP and how to use the results for further LTE studies of monopile-based support structures.

The flowchart in Figure 3.1 explains the steps taken in the investigated approach and how different parameters influence the results. Input parameters (parallelogram boxes) are divided in design and environmental parameters. Environmental parameters can have a direct or indirect influence on the PCs, which are fitted to measurement data for further estimations on lifetime. Oval boxes show intermediate results for further applications and final results: lifetime of CP systems and MP lifetime. One challenge is to adjust the PC and compare simulation results with measured potentials; the rhombus shape illustrates the decision on ***fit*** or ***no fit***. The best fitting curve is then implemented to analyze lifetime of CP systems, either directly by means of COMSOL Multiphysics® or by hand (dashed line gray boxes) with the simulation output I_{out} and the rearranged equation mentioned from DNV (c.f. Equation 2.15).
Furthermore, simulated potential distributions over the whole MP can help to identify, if parts of the structure might not be protected and to further localize unprotected parts.
Finally, the analyzed service life of CP systems is applied to decide which SN-curve, FC or CP, is needed to further estimate on MP lifetime by means of load analyzes.

In this chapter the applied methodology is introduced with its focus on GACP systems, internally and externally of a MP structure, based on measurement data provided from three different wind farms located in the North Sea.

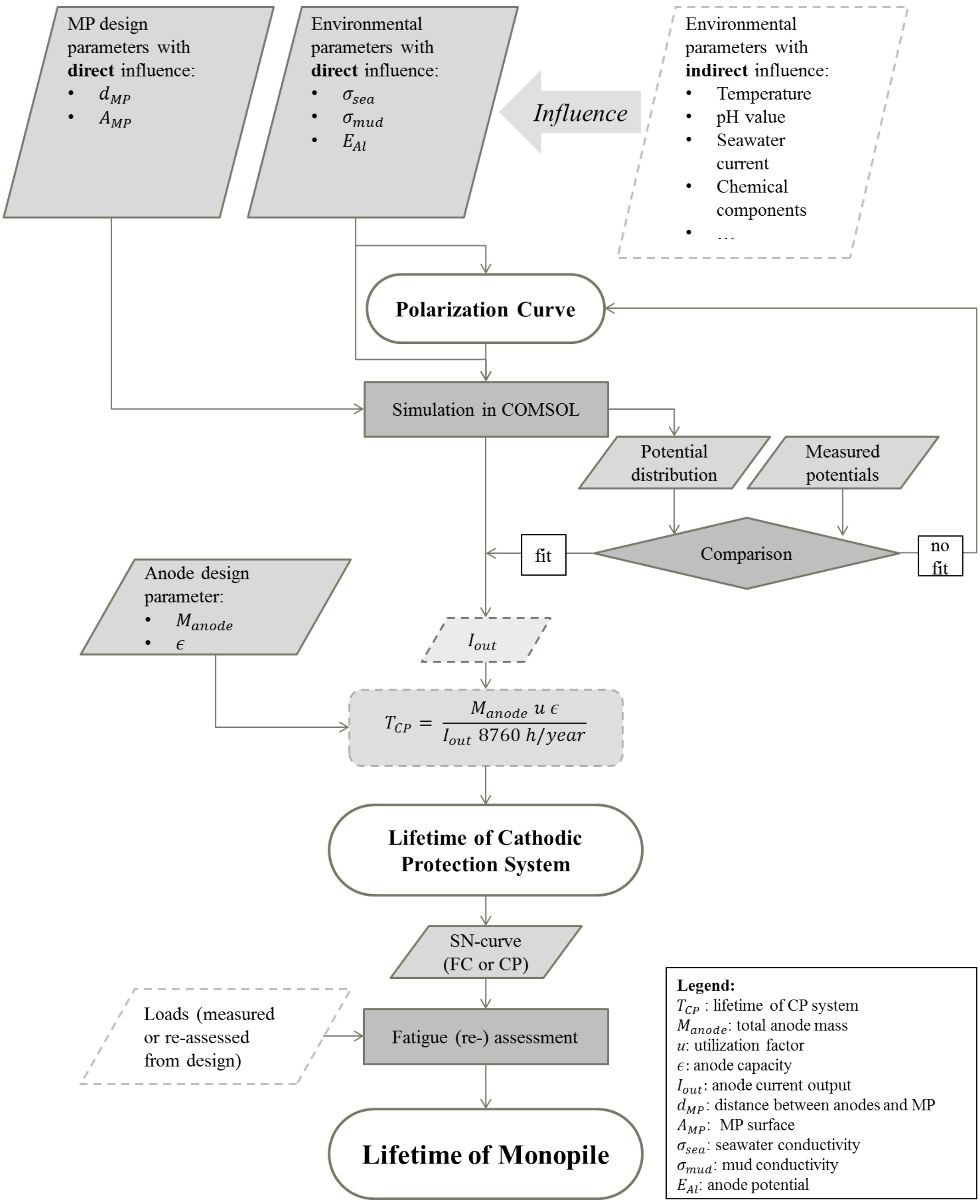

Figure 3.1: Flow chart of the investigated methodology

3.1 Requirements to prolong Service Life of CP Systems

Corrosion control systems for OWTs are difficult to inspect due to their offshore location. Inspections by divers or the deployment of remotely operated vehicles (ROVs) under water would lead to enormous costs and risks. However, the CP system must be assessed to estimate on LTE for offshore structures [1].
The approach taken in this study implies the corrosion simulation software COMSOL Multiphysics®, which is able to calculate current and potential outputs from corrosion protection systems applying kinetic expressions. Design assumptions, like MP geometry and material, anode specifications, and location of anodes have to be established from codes, standards, or design reports. Measured potentials are required to fit suitable PCs explaining the specific corrosion kinetics. Environmental parameters are needed to calibrate the simulation model to realistic conditions. Expert opinion is inquired if data or design assumptions are missing or afflicted with uncertainties or errors. Simulation outcomes are compared with the design to reassess lifetime. However, for precises prediction robustness of results should be verified.
If measurements are missing or confidential, a generalized data set based on experiences could be applied to perform a comparison between simulation and data.

3.2 On-site Measurements

In order to calibrate the simulation model, on-site measurement data from different OWFs are applied. These data contain electrical potential measurements as a function of water depth, from seawater surface down to the mudline and are partly supplemented by environmental data, like seawater conductivity, temperature, and salinity. To measure the potential a reference electrode (c.f. Section 2.8.3), electrically connected to the MP, is lowered down under water as close as possible to the MP surface. Measurements were either made by $Ag/AgCl^-$ electrodes or, if a $Cu/CuSO_4$ electrode was applied, the potentials are adapted by adding $-0.05\,V$ to allow for comparison.
Anchors and guide cables can produce relief to submerge the reference electrode uniformly and avoid drift aways by seawater current and tide. Alternatively ROVs equipped with reference electrodes can be implemented as well as professional divers. Under ideal conditions the potential field sent out from the anodes is recorded by the reference electrode directly at the MP surface. If the electrode comes too close to the anodes, it can happen that an open circuit potential very close to the anode potential is measured, which distorts representative information regarding protection potential at the MP. Any measurement outcomes nearby anodes should be treated with caution.

Several sensors or measurement buoys and masts provide environmental information on e.g.:

- seawater conductivity,
- salinity,
- water temperature,
- pH value,
- seawater current, or
- other chemical components.

Some parameters, like seawater conductivity (or salinity and temperature, which can be used to calculate specific seawater conductance [3]) and soil conductivity are required for evaluation. However, in case of missing or unclear data expert opinion allow for reliable assumptions. pH value and other chemical components are just nice to have for further interpretation of the results or for an advanced 'tertiary current distribution' model in COMSOL Multiphysics®.

It should be noted here that manual on-site measurements are usually taken during summer periods when the seawater has warmer temperatures and consequently a higher seawater conductivity. Measurement data should be treated with respect to environmental conditions. Shrinking calcareous deposit and absent marine growth as well as lower seawater conductivity (due to decreasing temperatures) during winter seasons could lead to poorer performance of corrosion protection systems.

3.3 Model Set-up

A simplified geometry of the MP is built in COMSOL Multiphysics® including anodes and electrolyte (seawater and soil). In 'Global definitions' input parameters are set and functions are generated to describe the kinetic expressions. Material properties are chosen for electrolyte and MP surface.
For the external CP model seawater and mud are built around the MP shell with a huge radius (100 times bigger than MP radius) and infinity conditions cylindrically and downwards in soil. In the internal CP model seawater and mud as electrolytes are limited by the inner MP circumference. Downwards in soil the infinity condition is applied.
In the selected interface 'secondary current distribution (siec)' the physic boundary conditions are defined. Electrolyte (seawater and mud), insulation and initial values are set as well as sacrificial anodes (as edges) and the MP as an electrode surface with its potential. In the latter, kinetic expressions are implemented to describe the electrode reactions on the MP surface (cathode). Kinetic expressions (PCs) are chosen from several predefined curves and user-defined functions (set in global definitions). The kinetic expression for anode edges is set as a predefined Buttler-Volmer function.

In the next step the mesh is created for all model components. For the anode edges an user-defined 'free tetrahedral' mesh is applied with a maximum element size of 0.1 m, all other edges are meshed with an 'extremely fine' 2D mesh (0.028 to 2.8 m). For the general physics a 2D mesh (min. element size of 0.05 m to max. 12 m) is set manually. The number of DOFs in the calculated model is around 11,000 and the simulation time for one stationary case is 4 seconds. Results with finer meshes (higher number of DOFs) require exceedingly more simulation time (c.f. Figure A.1 in Appendix A), but provide no surplus benefit regarding measurement accuracy and application for the investigated methodology of lifetime prediction. Potential accuracy in this thesis is set to five thousandth volts (0.005 V). Furthermore, time-efficient approaches are strove considering the planned methodology including time dependent studies and sensitivity analyzes for various GACP designs in different wind farms.

The time dependent study is applied to account for changes over years. Time steps are set individually (externally: years / internally: 0.01 years). In the post-processing step results (current and potential distribution, anode size, etc.) can be shown in various ways, e.g.: 2D graphs, visualized plots and videos, tables or single values. Outcomes (potential distribution as a function of water depth) are further processed in MATLAB®.

3.3.1 Input Parameter Set-up

Input data are divided in environmental parameters (measured or assumed) and design values for the support structure and protection system dependent on conditions, type, and requirements.
The MP structure geometry varies for different turbine sizes and locations in diameter and length. Additionally to the water depth, possible scour or soil push-up should be considered. The anode location is documented in design reports and drawings, but can also be stemmed from measurement data. Anode specifications are given by anode suppliers. Number of anodes, size (length, circumference, and inset radius), material density, and capacity must meet the requirements from DNV GL [3, 23].

- The **anode capacity** ϵ is usually given in ampere-hour per kilogram [Ah/kg], but has to be rearranged for COMSOL Multiphysics® in a value with the unit ampere-hour per meter [Ah/m]. This is done by multiplying the capacity ϵ in [Ah/kg] with the anode density and ring face of the anode [m^2]:

$$Q\,[\frac{Ah}{m}] = \epsilon \cdot \rho \cdot \pi(r_0^2 - r_{final}^2) \tag{3.1}$$

  where:
  ϵ = anode capacity $[\frac{Ah}{kg}]$
  ρ = density of anode material $[\frac{kg}{m^3}]$
  r_0 = initial anode radius $[m]$
  r_{final} = final anode radius $[m]$

  For a non-circular anode cross section the initial anode radius r_0 is [3]:

$$r_0 = \frac{c}{2\pi} \tag{3.2}$$

  with c as the cross section periphery in [m] [3].

- Anode potential and steel potential E_{Fe} are defined material specific. However, in COMSOL Multiphysics® the **input aluminum anode potential** E_{Al} can be set user-defined and is called anode equilibrium potential $E_{Eq,Al}$. Variations of input anode potential E_{Al} account for possible defects or inequalities in anode material composition.

- Environmental parameters contain **seawater conductivity** σ_{sea}, which can also be determined by salinity and water temperature by means of a diagram showing seawater resistivity over temperature and salinity in RP-B401 from DNV [3]. In case of missing measurements of seawater conductivity or salinity and temperature, assumptions can be made based on knowledge on location and season.

- Another parameter is the **soil conductivity** σ_{mud} which depends on the soil type and is therefore also related to the geographic location. σ_{mud} is chosen based on literature and experiences, e.g. according to DNV [3].

- **Scour** can occur externally and reaches values of 1.6 times the MP diameter in depth and a radius of 1 to 2 times MP radius, according to design reports. A soil push-up around the MP is illustrated by negative scour values. Soil push-up is mainly expected internally occurring from the ramming to install offshore MPs, but is not considered here.

- The **PC slope in mud** i_{mud} is set as a variable parameter to account for uncertainties due to missing measurements in soil. Value assumptions are following from codes and experiences [3].

Typical value ranges for the parameter set-up are listed in Table 3.1 according to literature, e.g. [3, 28], expert opinions, and design reports.

Table 3.1: Ranges for model input parameter according to DNV [3] and NACE [28], expert opinion (EO), and design reports (DR).

Parameter	Unit	Internal	External	Reference
E_{Al}	V	-1.0 to -1.1	-1.0 to -1.1	[3, 28]
ϵ	Ah/kg	1750 to 2750	1750 to 2750	[3, 28]
σ_{sea}	S/m	2.9 to 5.1	2.9 to 5.1	[3], EO
σ_{mud}	S/m	0.4 to 1.5	0.4 to 1.5	[3], EO
i_{mud}	$A/m^2/V$	0.005 to 0.025	0.005 to 0.025	[3]
scour	m	0	-1 to 6	DR

It should be noted here that several parameters are interacting with each other and some parameters are not directly implemented as a model input in the simplified 'secondary current distribution model' in COMSOL Multiphysics®, but nevertheless could effect the corrosion behavior of the system, e.g.:

- pH value,
- oxygen content,
- calcareous deposit formation, and
- other chemical components.

The following parameter are determined as fixed inputs to the simulation based on design and specifications. Variations in their settings would influence the results:

- distance from anode to MP surface d_{MP},
- protection potential ($-0.8\,\mathrm{V}$),
- potential of steel (*here: MP surface* $E_{Fe} = -0.6\,\mathrm{V}$),
- internal soil push-up or drilling depth, and
- all anode and MP specific design values (size, mass, surface area etc.).

Kinetic expression are input equations and can be set individually dependent on the regarded application. The next section gives an introduction on expression settings applied in the investigated studies.

3.3.2 Kinetic Expression Set-up

Kinetic expressions are defined by PCs, which show the required current density to provide a specified protection potential. The curves represent steady-state polarization conditions, where a stabilized phase is assumed when measurements are taken. Based on theory as well as laboratory, field experiences, and expert opinions different cathodic curve shapes are applied for corrosion in seawater. Outcomes will be compared to verify robustness.

Figure 3.2 shows schematic PCs applied to describe the kinetic expression in three different cases: **(a) linear**, **(b) piecewise (pw)**, and **(c) Tafel**. The x-axes show the current density from 0 to $0.1\,\mathrm{A/m^2}$, the y-axis starts from steel potential ($-0.6\,\mathrm{V}$ [47]) to the limiting protection potential ($-1.1\,\mathrm{V}$ [3]) before overprotection occurs. Table 3.2 lists the corresponding equations.

Table 3.2: Equations for kinetic expressions for cathodic polarization (*index c*): **(a) linear**, **(b) pw**, and **(c) Tafel** with PC slope in seawater i_{sea} in $[A/m^2/V]$, overpotential η_c and Tafel slope A_c in [V], scaling factor k, and cathodic current density i_c in $[A/m^2]$.

(a) linear	**(b) pw**	**(c) Tafel**
$i_c = \frac{i_{sea}}{0.3V} \cdot \eta_c$	$i_{c,1} = k \cdot \frac{i_{sea}}{0.1V} \cdot \eta_c$ $i_{c,2} = k \cdot \frac{i_{sea}}{0.35V} \cdot \eta_c + i_{c,1}$	$i_c = i_0 e^{\frac{\eta_c}{A_c}}$

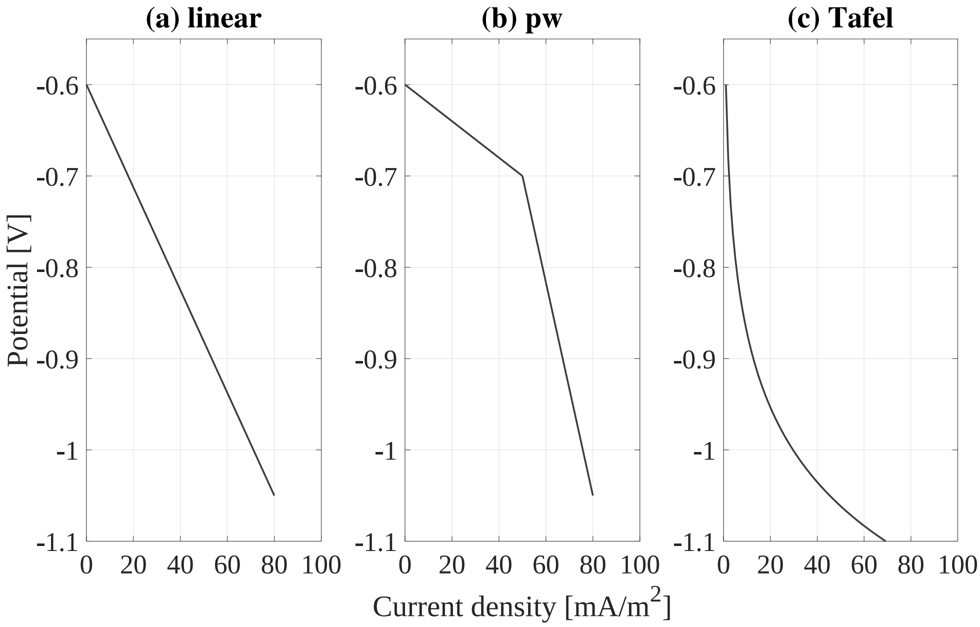

Figure 3.2: Schematic kinetic expressions for: **(a) linear**, **(b) pw**, and **(c) Tafel**. Protection potential at MP surface in $[V]$ over current density in $[mA/m^2]$.

(a) The **linear** curve is a simplification of the kinetic expression assumed in seawater, but meets protection current requirements calculated from traditional methods according to DNV [3]. In codes a specific value is determined, at which a maximum current density should be provided. In this case $-0.9\,\mathrm{V}$ is the protection potential at a current density of i_{sea} [3]. To reach the required slope i_{sea} must be divided by the factor $0.3\,\mathrm{V}$.

(b) The **pw** curve has two different slopes, which are both behaving similar to the linear curve. This simplification is based on theoretical steady-state PCs reflecting the potential-current interrelation for different anode designs according to Hartt [19, 21]. Long-term PCs run an invert S-shape (sigmoidal) curve illustrating the initial phase (high current output), formation of calcareous deposit (small current output), and possible break-down of deposit layer (increasing current output). However, the pw curve is expected to be stabilized shortly somewhere after protective calcareous deposit formation. The point where PC slope changes is fixed to $-0.7\,\mathrm{V}$, based on expert opinion.
The range from -0.6 to $-0.7\,\mathrm{V}$ is expected to have a flatter slope, which means that a higher increase in current density is needed to provided slightly more negative potential. In the second part of the pw curve, calcareous deposit formation is finalized and the slope is much steeper. Therefore, a small rise in current density results in stronger increase in negative potential. The scaling factor k is chosen in a way that requirements from traditional calculations are fulfilled.

(c) The **Tafel Equation** is a theoretical approach using a logarithmic expression, as explained in Chapter 2.2, Equation 2.9. A Tafel expression generally explains corrosion kinetics with hydrogen production, which can occur several meters below mudline, where no oxygen is present. The Tafel slope can also be valid for steel in acidic solutions (low pH values). However, since oxygen is present in seawater, evaluations with the Tafel slope expression should be regarded with caution, since consideration of oxygen availability and calcareous layer is neglected.

The PC in mud is set equally to the linear curve in seawater, but with a predetermined slope, providing $0.02\,A/m^2$ at $-0.9\,V$. In this thesis the PC slope in mud i_{mud} is treated as a varying parameter, as explained above, but not applied for PC fitting.
Theoretically, the Tafel slope expression might be relevant for surfaces in soil where hydrogen evolution is the governing cathodic reaction. However, this is out of scope of the thesis.

3.4 Polarization Curve Fitting

PCs are applied to evaluate the current reaching the MP surface. The challenge in this thesis is, that only potential measurements over the MP height are available, but current measurements are missing. Current density data would have allowed for a direct development of PCs and that could have led to more precises simulation of CP system performance.

Before the actual PC fitting starts, the **base case (bc)** of the model has to be set. Environmental data, either measured or assumed, are applied to calibrate the model most realistically. Parameters might be afflicted with uncertainties, which will be further assessed in local sensitivity studies.

Different PC types, mentioned above, are implemented to express the corrosion kinetic in the first simulation set:

- (a) linear,
- (b) pw, and
- (c) Tafel slope.

For each PC a simulation runs individually in its bc resulting in a **potential over height** (PoH) distribution as a function of water depth. Outcoming potentials from each simulation with a different kinetic expression will be compared to measurements. By iterative adjustment of the kinetic expression parameters (i_{sea}, k, and A_c, i_0) each simulated potential distribution is adjusted until it matches the measured potentials. i_{sea} and k are ranged from minimum to maximum values set according to expert opinions, listed in Table 3.3.
Adapted PC parameters should stay within their physically reasonable ranges.

The best match of PC parameters in each case is kept as a bc for further (lifetime) evaluations. This bc consists now of implemented measurement data, well justified

Table 3.3: Maximum (max) and minimum (min) PC parameters for internal and external GACP systems with PCs: **(a) linear**, **(b) pw**, and **(c) Tafel** slope.

PC slope	Parameter	Unit	internal	external
(a) linear	$i_{sea,min}$	$A/m^2/V$	0.095	0.025
	$i_{sea,max}$	$A/m^2/V$	0.005	0.001
(b) pw	k_{min}	-	0.1	0.1
	k_{max}	-	1.9	2.5
(c) Tafel	$A_{c,min}$	V	-0.28	*N/A**
	$A_{c,max}$	V	-0.1	*N/A**
	$i_{0,min}$	A/m^2	0.0001	*N/A**
	$i_{0,max}$	A/m^2	0.01	*N/A**

**N/A: no simulations performed*

assumptions, and an appropriately matched PC.

It should be noted here, that this method regards the PC fitting in mud with minor awareness, since potential measurements in soil are lacking. However, for realistic predictions, evaluation and influence of soil conditions are highly recommended. To account for uncertainties related to soil sensitivity studies are performed for varying PC slopes in soil (i_{mud}).

3.5 Evaluation of possible LTE for Monopile-based OWTs and its Robustness

The results on CP lifetime are regarded for further evaluations on the service life of a MP. It should be noted here, that the critical point for fatigue failure at the MP can differ from the hotspot where cathodic corrosion protection fails first. Analyzes of CP performance life allow to decide, which of the two different SN-curves (FC or CP, c.f. Section 2.4) applies to estimate the lifetime of the MP at its critical spot by means of Miner's Rule (c.f. Equation 2.11).
When a corrosion protection system reaches its lifetime and fails to protect the whole structure, FC must be assumed. Hence, MP lifetime evaluations must be done by applying SN-curves for FC, which than in turn have shorter service life expectations compared to SN-curves with a fully working CP system.
Usually external GACP systems are designed for the same lifetime than MPs, whereas internal GACP systems have shorter services lives due to their interchangeability.

3.5.1 Lifetime Analysis of GACP Systems

The determined bc explained in the previous section is used to evaluate the total useful lifetime of a GACP system. Potentials more negative than a defined threshold value ($-0.8\,V$ [3]) are providing full corrosion protection. By reaching less negative potentials at any point of the MP surface, full protection would be endangered and thereby the MP surface would be exposed to FC, which could lead in reduced lifetime. The critical point of CP is depending on the design (mainly anode location and distance) and is usually farthermost from the anodes. By looking at the simulated potential distribution over the MP that point can be identified. To estimate on service time the COMSOL Multiphysics® simulation runs over a defined time range and calculates the potential distribution for each time step taking into account anode consumption. The last date (externally in years / internally in 0.1 years) when $-0.8\,V$ is still provided at all spots, is the total CP lifetime of this simulation set-up.

To investigate robustness of results a comparison with additional measurement data from a second year is done. Furthermore, the local sensitivity of results on different input parameters (discussed above) is estimated by ranging one parameter at the time and identify whether the influence on the resulting lifetime is strong or weak. By doing so, a worst and best case scenario is generated for each parameter. For the worst case each parameter is set to the value resulting in the shortest lifetime, for best case, the values with the highest lifetime outcome are picked. It should be noted here, that the lifetime resulting from best case can be shorter than the bc and vice versa, the worst case can result in longer lifetime than the bc. This recognition can be explained by the interaction of parameters between each other. Global sensitivity studies would account for parameter interaction but are not evaluated in this scope.

COMSOL Multiphysics® calculates the average current density of the MP area in seawater directly. If the MP is fully protected at each point, the average current density over the whole submerged MP surface is calculated as:

$$i_{av} = \frac{I_{out}}{A_{sea}} \tag{3.3}$$

where:
A_{sea} = submerged MP surface area $[m^2]$
I_{out} = total current output from all anodes $[A]$

Average current densities can be compared to design values provided in design reports. If i_{av} values are smaller than mean values from design, the CP system was design conservatively and extension of CP performance might be feasible. Values higher than the design current density indicate a higher anode consumption, which leads to faster depleting anodes and with that to shorter lifetimes.

3.5.2 Lifetime Analysis of ICCP Systems

Voltage and current output measurements from ICCP systems can be used to evaluate the average current density i_{av} by hand. This is realized by estimating a mean and initial current value [A] from data series over time recorded at different turbines and applying Equation 3.3 (c.f. Section 3.5.1). In case of a potential controlled ICCP system and if full protection at each point of the structure is assumed, the average current density can be compared to recommended values in codes [23]. Additional assumptions could be e.g. equal environmental parameters (same location), which would allow for a complementary comparison with GACP results.
Furthermore, design assumptions for ICCP anodes can be tested, e.g. maximum anode current and anode material consumption.

4

Results and Discussion

In consideration of the introduced methodology the following results are discussed in this chapter:

- lifetime evaluation of GACP systems inclusive related sensitivity and robustness,
- data analysis from a potential controlled ICCP system,
- limitations to be considered for result evaluation, and
- significance and application for existing OWFs as well as industrial implementation and environmental aspects.

For each evaluation one or more turbines are randomly picked from the provided measurement data and are numerated in this thesis from 1 to x (x: number of analyzed turbines). This is a fictive numeration which is not related to the original wind park (WP) configuration. Data is provided from wind farms which are equipped with internal and external CP systems. WPs with GACP systems are numbered with A and B; the wind farm operating an ICCP system is here called WP C.
Data is applied and evaluated as explained in Chapter 3 to estimate on performance of CP systems as well as on robustness of simulation and measurement outcomes. CP performance fails if required protection potential at any point of the structure surface is missing. The point where CP fails first is usually farthest away from the anodes. In WP A this point is internal as well as external at the mudline. WP B has its external critical spot also at the mudline, but internally the hotspot is some meters below TB.
There are two possibilities of a failing CP system:

1. anodes are depleted,
2. anode current output does not reach the MP surface at any point of the MP surface, due to several aspects (e.g. high seawater resistivity, interference between anodes and distance to MP surface, anode potential).

Which case occurs is mainly dependent on the design, but is also affected by environmental conditions. Regarding possible LTE of the monopile-based support structure the reason for missing corrosion protection is subordinately. However, if it comes to retrofitting and improvement of CP systems as well as lifetime-extending interventions at the support structure the failure origin becomes significant.

4.1 GACP

Design and measurement data from WP A and WP B (internal and external) and additionally several recorded environmental parameters are available. The approach illustrated in the flowchart in Figure 3.1 is applied for lifetime evaluation of GACP systems. Coating is internally negligible in both wind parks. Externally the MP is partly coated (40 to 50% of MP surface) and a mean coating breakdown factor according to design is applied for simulations.

4.1.1 Model Calibration and Parameter Influence

To start lifetime evaluation, a bc is set by **calibrating** a simulation model with measured and assumed **(environmental) parameters** and **design values**. Potential of aluminum anodes, anode capacity, scour, as well as seawater and mud conductivity show different effects on the outcoming potential distribution.

- Variations in **aluminum anode potential** E_{Al} account for uncertainties related to anode design and manufacturing. Adjustments of E_{Al} (to more or less negative values) shift the potential distribution along the MP height to more or less negative potentials. The input value of E_{Al} could be precisely measured with reference electrodes close to the anodes.

- **Anode capacity** ϵ is chosen from the RP according DNV [3] or design reports. This suggestions might be conservative and therefore it can be expected that ϵ is higher in reality. Changes in ϵ do not effect the protection potentials directly, but have a major influence on the lifetime of a CP system. Lifetime increases linear with higher capacities due to higher ampere-hour values per kg anode mass (c.f. Equation 2.15 in Chapter 2).

- Conductivities are depending on location specific environmental conditions. **Seawater conductivity** σ_{sea} is either measured on-site or can be determined by known temperature and salinity values. Low seawater conductivities impede that parts from the MP (most far away from anodes) can be out of reach of current emission from anodes. This would lead to a failing protection system, even though anodes still exist. Higher seawater conductivities might ensure that current reaches all parts of the structure, but in turn anodes are also consumed faster.
  A large **mud conductivity** σ_{mud} results in an increased current drain in mud. Current drain in mud is externally higher than in the inner MP due to a larger reachable area (seabed around MP) - internally the area, where current can drain in, is limited by the inner MP cross section.
  Both conductivities can be afflicted with uncertainties due to measurement errors, poor measurement equipment, and lacking data.

- **Scour** expands the MP surface and increases the distance between anodes and mudline, which can lead to unprotected parts of the structure when ML is the critical spot and small σ_{sea} values.

- The **PC in mud** i_{mud} depends on soil type and conditions. Increasing i_{mud} values would lead to a flatter PC slope in mud, and with that to a higher current requirement.

The simulation model is calibrated to measured data from WTG 1 in WP A. Inputs are listed in Table 4.1; values in the column 'range' show the physically reasonable range in which the bc might occur, according to Table 3.1 in Chapter 3.

Table 4.1: Design values and input parameters in bc and ranges for internal and external GACP simulations for WP A.

Parameter	Unit	Design	internal		external	
			bc	range	bc	range
E_{Al}	V	-1.05	-1.075	-1.0 to -1.1	-1.075	-1.0 to -1.1
ϵ	Ah/kg	2000	2000	1750 to 2750	2000	1750 to 2750
σ_{sea}	S/m	3.33	4.7	2.9 to 5.1	4.7	2.9 to 5.1
σ_{mud}	S/m	0.67	0.7	0.4 to 1.5	0.7	0.4 to 1.5
scour*	m	-1*	0	N/A**	0	-1 to 6

**only relevant for external cases*

***N/A: no simulations performed*

4.1.2 Polarization Curve Fitting

The bc determined in Section 4.1.1 is the basic setting for the following **PC fitting** by adjusting **PC slope parameters** i_{sea} for **(a) linear**, scaling factor k for **(b) pw**, as well as A_c and i_0 for the **(c) Tafel** slope.

Figure 4.1 shows PoH plots for an internal GACP system and Figure 4.2 for an external GACP system in WP A. Negative potentials are plotted on x-axis from $-0.6\,V$ to better protection (max. $E_{Al} = -1.1\,V$). Normalized water depth is shown on y-axis from MSL down to mudline (in plots: ML). For missing design data water depths and anode positions are suggested based on measurements.

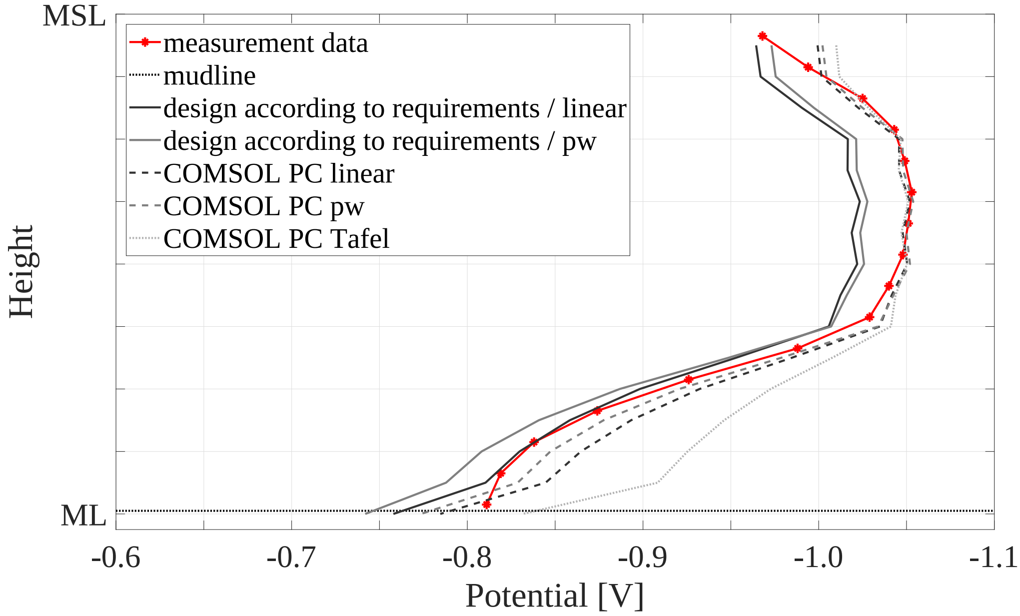

Figure 4.1: PC fit for an **internal** GACP system in WP A to measurement data (red dots with interpolated line); design PoH progress for linear (dark solid line) and pw PC slope(bright solid line) according to requirements and after model calibration to measurement data with PC slope: **(a) linear** (dark dashed line), **(b) pw** (bright dashed line), and **(c) Tafel** (bright dotted line).

From Figure 4.1 it can be seen, that **internally** simulated PoH curves according to requirements without calibration and fitting (solid lines) give less negative potentials, compared to measurements (red asterisks connected with a red solid curve) which are showing higher protection potentials. By calibration of all parameters to bc conditions, both solid curves (**(a) linear** and **(b) pw**) are moving to more negative potentials, closer to the measurement points. A good match is already given before a fitting of the PC slope is performed, which means that i_{sea} stays in its design value for linear PC and the scaling factor k is 1 (no scaling). In this special case, calibration to environmental data shows a good match to measured potentials and no further PC fitting is necessary.
The difference between a simplified approach of a linear PC slope shows only minor changes to the approach by using a pw PC slope. However, it should be noted, that the pw PC slope accounts for a more realistic progress, but is afflicted with additional uncertainties due to its inflexion point set to $-0.7\,\mathrm{V}$.
An adjustment with the **Tafel** equation corresponds quite well to measurement data with an implemented parameter set-up of $A_c = -0.23\,\mathrm{V}$ and $i_0 = 0.001\,\mathrm{A/m^2}$. However, A_c values recommended in literature are around $-0.1\,\mathrm{V}$ [35], which is 50% less than the fitted value and is therefore not in a reliable range. That could be explained by the fact, that the Tafel equation is usually implemented for hydrogen evolution corrosion, but in seawater an oxygen driven corrosion is predominated.
Matching closer to the mudline becomes more difficult. This phenomena is explainable by the assumed PC in soil, which is simplified to a linear PC slope (i_{mud}) due

to missing data in mud.

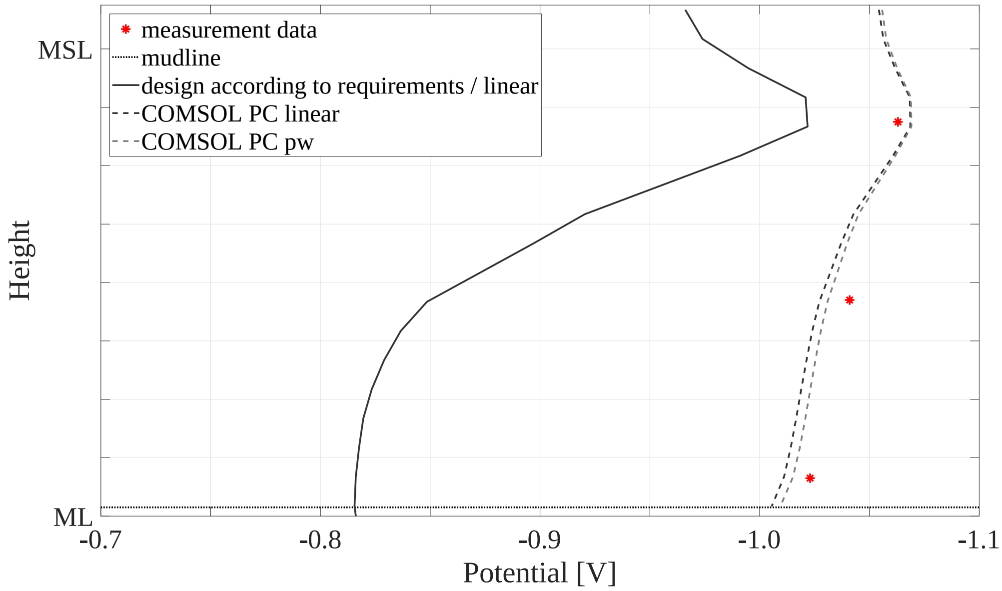

Figure 4.2: PC fit for an **external** GACP system in WP A to measurement data (red dots); design PoH progress for linear PC slope (dark solid line) according to requirements and after model calibration and PC fitting to measurement data with PC slope: **(a) linear** (dark dashed line), **(b) pw** (bright dashed line).

The PC fit for an **external** GACP system is plotted in Figure 4.2. The red asterisks are the measurement points at an upper, middle, and lower position suggested 1 m below seawater level during measurement, half way down to mudline, and approximately 1 m above seabed. Exact elevations are not known.
The designed PC (linear) is less negative than the actual measurements. After calibrating all environmental parameters and fitting of PC slope values i_{sea} (linear) and k (pw), the current density is around 10 times smaller than the design value (for **(a) linear** and **(b) pw**), which is surprisingly small. Low current requirements at the MP surface lead to slower depleting anodes than accounted for. This, in turn, results in longer lifetimes of the CP system compared to the design lifetime (here: around 10 times longer), on the prerequisite that actual conditions, implemented for calibration and fitting, stay constant in future. Assuming that results are right, that would indicate a conservative design regarding anode size and mass, which could be reduced in future applications for new wind farms to save on material costs.

However, PC fitting is quite uncertain, since only three measurement elevations per OWT are available and thus results should be treated with caution. Further analyzes are recommended, implementing more potential measurement points and certain data.
The Tafel slope fitting is skipped for external analyzes, since preceding results showed an unreliable application.

Additional simulation outcomes show that a high potential drop to steel potential (-0.6 V) occurs in soil (internal higher than external), which in turn leads to a marginal current requirement below seabed. That can be caused by a high soil resistance (low soil conductivity). Furthermore, negligible oxygen content in deeper soil might inhibit corrosion progress at the buried MP surface.

The same approach of PC fitting with **(a) linear** and **(b) pw** is applied for **WP B**; plots are attached in Appendix A Figure A.3 (GACP internal) and A.4 (GACP external).

The resulting **internal** current density is for the regarded turbine higher than the design requirements. Thus, lifetime of the internal CP system would be shorter than designed for. Internal CP systems from other WTGs in WP B show similar problems, but others also show decreasing current densities. That could be due to different dates (differing environmental conditions) when measurements have been done, but also due to changes in the design for internal CP systems within WP B. From Figure A.3 it is also seen, that a fitting to the three measurement points is very difficult. This could have several indicators, like large measurement scatters regarding the measurement elevation or uncertainties from environmental parameter calibration.

Simulation outcomes for **external** GACP systems in WP B, after calibration to environmental data and fitting to potential measurements, are similar to results in WP A. The current density is around 10 times smaller compared to design expectations. This could be explained by a similar anode arrangement around the MP externally in both wind farms, although water depth is around 60% deeper in WP B.

The comparisons of internal CP systems between two wind farms but also between different WTGs within the same OWF show, that PoH measurements vary in large scatters. That could be caused by differences in anode arrangements as well as in MP designs, water depths, and environmental conditions.

4.1.3 Sensitivity Study: Robustness of Results based on Parameter Influence

Results based on measurement data (environmental data and PoH measurements) are afflicted with uncertainties. Furthermore, the approach of the PC fitting showed challenges finding proper matches of simulated and measured PoHs. Therefore, sensitivity studies are applied to

1. consider possible **measurement errors and variations** due to assumed values,
2. to account for **model uncertainties** (uncertainties from PC fitting).

4.1.3.1 Measurement Uncertainties: Influence of Environmental Parameters

Outcomes from sensitivity studies show how sensible CP lifetime predictions are to parameter variations, listed in Table 3.1 (c.f. Section 3.3.1). Lifetime deviation is plotted over parameter variation. The y-value 1 is the normalized lifetime when all parameters are set to their bc and the best match of PC fitting is determined (x-value = 1). This is illustrated with a red circle in all following figures. The steeper the curve progress, the more influence a parameter has on the results.
It should be noted here, that bc lifetime which is set by calibrated (environmental) parameters (c.f. Section 4.1.1) and fitting of PCs (c.f. Section 4.1.2), but not the design CP lifetime.

The following discussions are based on comparisons between different:

- PC fitting approaches: **(a) linear** and **(b) pw**,
- internal and external GACP systems (anode arrangement and designs),
- wind farms: WP A and WP B (location, design, ...), and
- possible hotspots (internally): mudline and close to TB.

Comparison of parameter influence from linear and pw PC fitting on an internal CP system
Figure 4.3 and 4.4 show parameter variations in WP A, internally at the critical spot (here: mudline), where protection is expected to fail first.

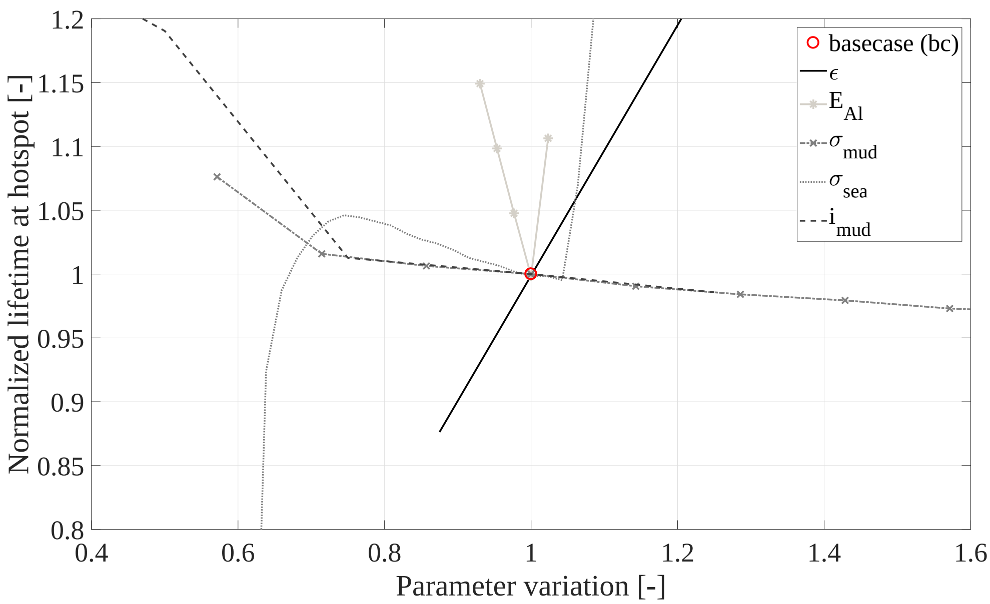

Figure 4.3: Normalized lifetime over parameter variations at the hotspot (here: mudline) of an internal GACP system in WP A with **(a) linear** PC slope.

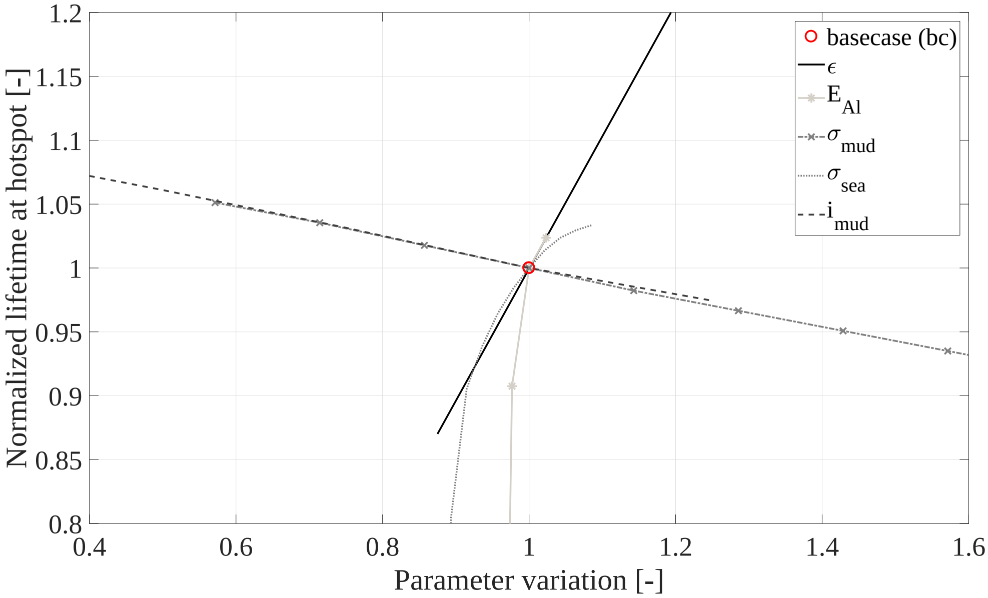

Figure 4.4: Normalized lifetime over parameter variations at the hotspot (here: mudline) of an internal GACP system in WP A with **(b) pw** PC slope.

- **Anode capacity** ϵ**:** Lifetime of CP is linear dependent on anode capacity in both approaches, linear and pw. As higher the capacity, as higher the lifetime, since more ampere-hours are provided per kilogram anode mass which leads to longer resisting anodes. A decreased capacity of 0.85 leads to 85% of lifetime. The same accounts for increased values: for the maximum ϵ value of (2750 Ah/kg) the lifetime is prolonged by 1.375.

- **Input anode potential** E_{Al}**:** Variations in E_{Al} for linear and pw show disparate changes in lifetime. In the linear case the progress has a V-shape and the smallest lifetime result lays at the bc (-1.075 V). Changes to smaller and higher anode potentials increase the lifetime to 115% for -1.0 V and 101.6% for -1.1 V. The curve behavior until bc might be caused by faster anode depletion in case of higher E_{Al} (higher anode current output). Increasing lifetime can be caused by a better protection from more negative E_{Al} values. However, the latter leads to a contradiction to the statement about the curve progress in the range from -1.0 V (0.85) to -1.075 V (bc).
  For the pw approach the curve runs down to zero years of lifetime for values less negative than -1.05 V. For -1.1 V the lifetime increases slightly to 102.4%. With increasing E_{Al} values the protection potential reaching the MP surface is more negative. In turn the protection potential is poorer with lower E_{Al} values leading to failing protection potentials (although anodes are still available).
  The curve progress in both cases, linear and pw, show inconsistent physical behaviors.
  However, uncertainties in E_{Al} follow from anode manufacturing and the scatter is usually small (0.1 V).

- **Seawater conductivity σ_{sea}:** Seawater conductivity shows a strong influence, especially when it comes to values below 3.5 S/m (linear) or values smaller than the bc 4.7 S/m (pw), where the lifetime drops down to zero. This is explainable due to a failing system, when current output from anodes does not reach the critical spot (here: mudline) anymore, even though anodes are still existing. The slight rise in lifetime at σ_{sea} values from 4.9 to 3.5 S/m in the linear PC approach might result from a slower depletion of anodes due to decreasing conductivity, but before conductivity is too small to reach the hotspot. An increase to 120% of lifetime is seen for σ_{sea} values higher than 4.9 S/m (linear case). The highest lifetime in the pw case results at maximum σ_{sea} and is 1.033 times lifetime. While the pw approach decreases continuously, for the linear case this failure occurs first for values smaller than 2.7 S/m, However, the linear case shows also increasing lifetime (0.995 to 1.046) for decreasing σ_{sea} from 4.9 to 3.5 S/m.
  Concluding it can be said, that both approaches show problems of protection potential reaching the critical spot for decreasing conductivities, which can either occur due to a poor distribution of anodes (design) or the applied methodology might be unreliable.

- **Mud conductivity σ_{mud}:** The influence of mud conductivity differs slightly between the linear and the pw approach. For both case a decreasing lifetime for higher σ_{mud} values is seen. High σ_{mud} values mean in turn low mud resistance values, which lead to a higher current drain in mud. With high current drain in mud, anode consumption increases and lifetime of CP is reduced. The slope for the pw method is steeper between the range 0.71 to maximum σ_{mud}. Values smaller than 71% σ_{mud} (0.4 and 0.5 S/m) show a faster increase in lifetime in the linear case, up to 107.6% lifetime. For the pw case the lifetime seems to decrease linear over the whole range from 87.0 to 105.1% of lifetime.

- **PC slope in mud i_{mud}:** The PC slope in mud shows a very similar progress to variations in σ_{mud} for both cases, linear and pw. A slight decrease in lifetime for increasing current drain in mud is seen. For the linear approach the lifetime starts to rise faster when i_{mud} is smaller than 0.015 A/m^2/V; similar to what was seen for mud conductivities.
  Small i_{mud} values can lead to longer lifetimes (127% linear and 109% pw). This phenomena might be caused by the same statement as discussed for mud conductivities: increasing current drain in mud (large i_{mud} values) lead to shorter lifetimes due to faster depleting anodes.

It can be summarized, that behavior of mud conductivity and current drain in mud (PC slope in mud) as well as anode capacity is similar in both approaches (linear and pw). Hence, it can be concluded that the simplified approach of a linear PC results in similar outcomes as the more advanced pw approach and therefore future analyzes on σ_{mud} and i_{mud} could be performed applying the linear PC approach.
Anode potential has a small variation range, but shows very different reactions in

lifetime evaluation for both cases, linear and pw.
Variations in seawater conductivity are inconsistent in both cases, but can be explained by the two different failure cases: (1) the linear PC approach is more sensitive to anode depletion, whereas for the pw approach even protection at all points of the MP surface fails before anodes are totally consumed (failure 2). Additional studies should be performed to identify why linear and pw approaches are sensitive to different failure cases, and if the simplified approach ((a) linear PC) is more precise than the pw PC approach, which could be due to additional uncertainties by setting the inflexion point. Furthermore, verification of the applied methodology is recommended to exclude a poor design of the GACP system.

Worst and best case scenario for internal CP system in WP A
For each parameter the worst and best case value is taken, for which the lifetime is highest in local sensitivity analyzes. Values in Table 4.2 are used to calculated on a worst and best case lifetime for the GACP system in WP A internally. It should be noted that global sensitivity studies could lead to different results regarding worst and best cases.

Table 4.2: Input parameters for worst, base, and best cases for an internal GACP system in WP A with **(a) linear** and **(b) pw** PC slope, and resulting lifetime deviation.

Parameter	**Unit**	**bc**	**(a) linear**		**(b) pw**	
			worst	**best**	**worst**	**best**
E_{Al}	V	-1.075	-1.075	-1.0	-1.0	-1.075
ϵ	Ah/kg	2000	1750	2750	1750	2750
σ_{sea}	S/m	4.7	2.9	5.1	4.0	5.1
σ_{mud}	S/m	0.7	1.5	0.4	1.5	0.4
i_{mud}	$A/m^2/V$	0.02	0.025	0.005	0.025	0.005
Lifetime deviation	-	1	0	1.67	0	1.52

Lifetimes in both worst case scenarios result in zero which might caused by a low seawater conductivity and with that anode current output is unable to reach the critical spot, as explained in failure 2. This statement can additionally verified by simulation which shows that anodes are still existing.
The best case for the linear PC slope approach results in 1.67 times bc lifetime. For the pw approach the best case shows 152% lifetime for the internal CP system. Those scenarios show, that the pw approach is more conservative, resulting in shorter best case lifetimes compared to the linear approach.

Worst and best case scenarios do not include variations in PC slope in seawater i_{sea}. Those model uncertainties will be discussed in Section 4.1.3.2.

Comparison of parameter influence from linear and pw PC fitting on an external CP system
Figure 4.5 and 4.6 show parameter variations for external GACP systems in WP A at the critical spot (here: mudline), where protection is expected to fail first. It can be seen, that in both plots progresses of all curves are almost identical.

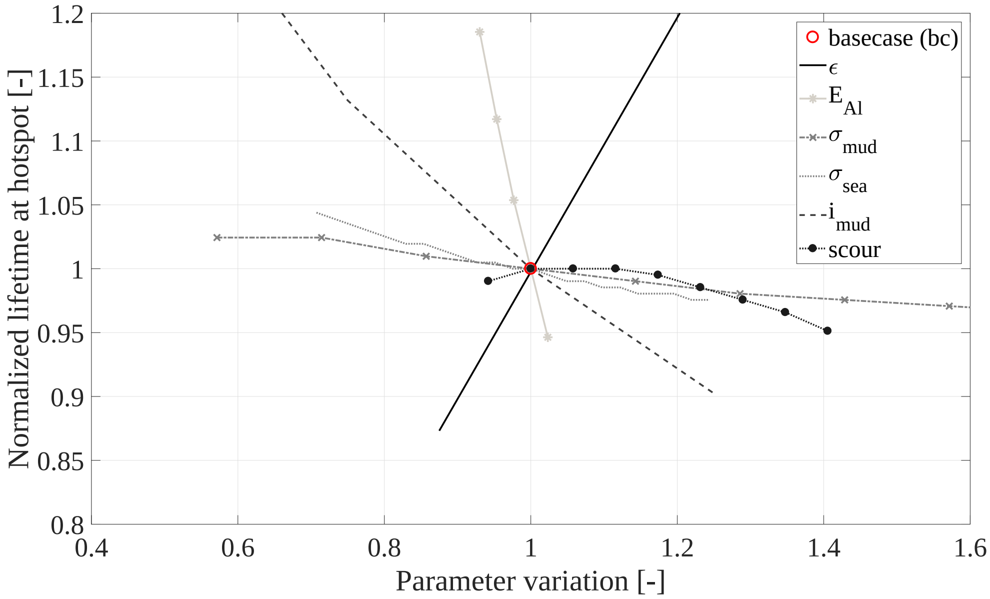

Figure 4.5: Normalized lifetime over parameter variations at the hotspot (here: mudline) of an external GACP system in WP A with **(a) linear** PC slope.

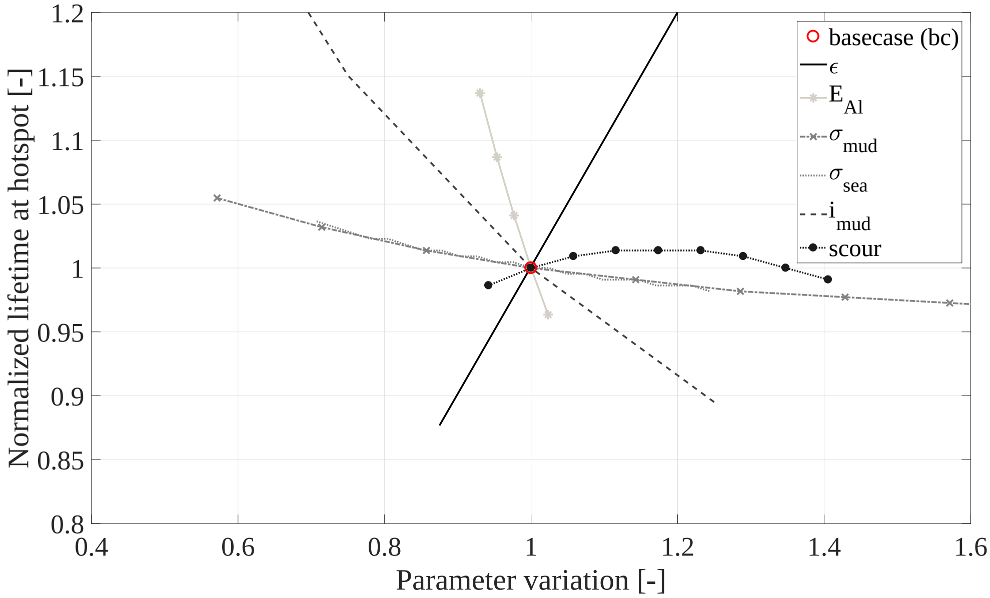

Figure 4.6: Normalized lifetime over parameter variations at the hotspot (here: mudline) of an external GACP system in WP A with **(b) pw** PC slope.

- **Anode capacity** ϵ**:** Parameter influence for anode capacity at an external GACP system equals the evaluation from internal GACP system, as explained above.

- **Input anode potential** E_{Al}**:** Variations in E_{Al} for linear and pw show the same progress in both cases. As more negative the anode potential, as shorter is the lifetime. That can be explained by a faster anode consumption for more negative anode potentials (higher current output). In the linear approach, resulting lifetime is longer for $-1.0\,\mathrm{V}$ and slightly shorter for $-1.1\,\mathrm{V}$. Hence, the sensitivity for the linear PC slope is marginal stronger than for the pw PC case.

- **Seawater conductivity** σ_{sea}**:** Seawater conductivity has a steeper curve than σ_{mud} in the linear case (104.4 to 97.6% lifetime) and a similar progress as σ_{mud} for the case with a pw PC slope (103.7 to 98.2% lifetime).

- **Mud conductivity** σ_{mud}**:** The influence of mud conductivity differs slightly from linear to pw approach. For both case a decreasing lifetime for higher σ_{mud} values is seen. From 71% bc to minimum σ_{mud} the lifetime stabilizes at 102.4% in the linear approach, but not in pw. For the pw case the lifetime decrease uniformly over the whole range from 105.5% to 95.9%.

- **PC slope in mud** i_{mud}**:** The PC slope in mud (linear) shows a very similar progress to variations in σ_{mud} for both cases, linear and pw. The influence in the linear method is slightly less sensitive (from 164.0 to 90.2% lifetime) compared to the pw PC approach (from 177.6 to 89.5% lifetime).

- **Scour:** The effect of scour results in a decreasing lifetime for the linear case. For 6 m scour the resulting lifetime is 95% since more surface has to be protected. The pw cases shows an increased lifetime due to scour till 5 m. For 6 m scour the lifetime is minimal shorter (99.1%). For negative scour/soil push-up (linear and pw), which means a lifted up mudline, the lifetime is also slightly shorter. That can be explained by the PC slope value in mud, which is (after PC fitting) higher than the one in seawater. Hence, the current drain seems to have a higher influence on lifetime than the surface area to protect, especially in the pw case.
  Effects of scour are highly recommended to evaluate in detail when measurement data from soil are available.

The comparison between the simplified linear and the more detailed pw approach for external CP systems shows only minor variations for all parameters. The linear PC might be a good simplification for further estimations on external CP systems with similar design and conditions.

Worst and best case scenario for internal CP system in WP A
Table 4.3 lists the worst and best case values for each parameter in WP A externally.

Table 4.3: Input parameters for worst, base, and best cases for an external GACP system in WP A with **(a) linear** and **(b) pw** PC slope, and resulting lifetime deviation.

Parameter	Unit	bc	linear		pw	
			worst	best	worst	best
E_{Al}	V	-1.075	-1.1	-1.0	-1.1	-1.0
ϵ	Ah/kg	2000	1750	2750	1750	2750
σ_{sea}	S/m	4.7	5.1	2.9	5.1	2.9
σ_{mud}	S/m	0.7	1.5	0.4	1.5	0.4
i_{mud}	$A/m^2/V$	0.02	0.025	0.005	0.025	0.005
Scour	m	0	-6	0 to -2	+1	-2 to -4
Lifetime deviation	-	1	0.71	2.76	0.68	2.74

Resulting lifetime for worst case scenarios is approximately 70% of bc lifetime. The pw approach results in a slightly smaller lifetime deviation.
The best case for the linear PC approach results in 2.76 times longer lifetimes compared to the bc lifetime. For the pw approach the best case shows 2.74 times increasing lifetime for the external CP system. Overall it can be said, that differences between linear and pw PC slopes are insignificantly small for external GACP analyzes. The simplified approach of linear PC fitting leads only to slightly less conservative results.

Comparison of parameter influence between internal and external CP systems

Since anode capacity influences the lifetime directly, the progress of its curve is similar in each comparison (c.f. Parameter influence on lifetime of internal CP).
Compared to the influence internally, lifetime changes due to σ_{sea} are very small externally. Failure 2 (non-reaching current at the hotspot) does not occur in the external GACP system. Variations in soil conductivity have nearly the same influence as σ_{sea}, internally and externally, especially in the pw case. Current drain in mud shows externally a higher sensitivity compared to internal systems. Changes in anode potentials externally show the same lifetime deviations with linear and pw PCs. The latter was not seen for internal analyzes, which could be explained by a different GACP design, but also by the PC parameter i_{sea}, which is internally 5 times higher ($i_{sea,int} = 0.01\,\mathrm{A/m^2/V}$; $i_{sea,ext} = 0.05\,\mathrm{A/m^2/V}$); pw scaling parameter k is 3.5 times higher for internal evaluation.
Mainly notable is that for external GACP the simplified approach of a linear PC fitting results in similar sensitivities, which is not seen for internal CP systems.
Different designs, anode arrangements and types, as well as conditions in the inner or outside of the MP might be the main factor for incompatible comparison between internal and external CP systems. Comparison between different anode designs and arrangements as well as applications (internal and external) are not recommendable.

Comparison of parameter influence on lifetime between external CP systems in different WPs (linear and pw PC slope)

The best fitted PC curve slope for WP B is given with an i_{sea} value of $0.01\,\mathrm{A/m^2/V}$ and $k = 0.1$, which equals the fitting from WP A. Anode arrangements in both OWFs are similar. The major difference between the two wind farms is the water depth; the mudline in WP B is about 60% deeper than in WP A. Furthermore, the GACP system in WP B contains more anodes and the total anode mass is higher, which can be related to the larger MP surface in seawater (due to the deeper mudline).

Plots for WP B are attached in Appendix A (c.f. Figure A.3, A.4, A.5, A.6, and A.7 to A.10).

- **Anode capacity ϵ:** Parameter influence of anode capacity is equal for both WPs in the linear and pw PC approach.

- **Input anode potential E_{Al}:** E_{Al} shows for the linear and the pw case, the same progress in both wind farms. In the linear approach lifetime deviation is more sensitive to variations in E_{Al}.

- **Seawater conductivity σ_{sea}:** Variations in σ_{sea} lead in the same curve progress and lifetime deviations for WP A and WP B for both PC fitting cases. Again the linear approach is slightly more sensitive to variations in seawater conductivity.

- **Mud conductivity σ_{mud}:** Mud conductivity shows for both wind parks a similar progress in both approaches (linear and pw). WP A is slightly more sensitive to variations in mud.

- **PC slope in mud i_{mud}:** The PC slope in mud shows a larger influence in WP A, whereas WP B has a smaller lifetime deviation due to changing i_{mud} values. This phenomena is seen in the linear and the pw case.

- **Scour:** Lifetime decreases strongly to 90.3% for deeper scour in WP B, since MP surface area increases with a deeper mudline. More current output is needed to protect the larger area from corrosion in seawater.

WP A is less sensitive to variations in seawater conductivity, but more to variations in mud compared to WP B. The biggest difference between the two wind farms is, that increasing scour results in rising lifetime for WP A, whereas in WP B the lifetime decreases constantly with larger scour depths. The phenomena seen in WP A could be explained by the mudline level, which is (at the regarded WTG) 60% higher compared to the WTG in WP B. Therefore current output at the MP in WP B might struggle reaching the critical point (deepest point) of the MP surface. Another explanation could be, that in the simulation model, PC slope in mud is assumed higher than in seawater, which would in turn lead to higher current requirements on surfaces covered by mud compared to surfaces exposed to seawater. However, this conclusion, based on simulation outcomes, would contradict the theory that corrosion in deep soil is insignificant due to missing oxygen content.
Apart from this, it is seen that variations in E_{Al} and σ_{sea} have higher influence on lifetime deviations in the linear approach for both external CP systems. As deeper the mudline, and with that as greater the submerged area, the influence of mud conductivity and current drain in mud becomes less crucial.

From this comparison, it can be said that similar environmental conditions, anode position and arrangement, and anode designs lead to the same influences on lifetime of external CP systems in the linear as well as the pw PC fitting approach on condition that anode mass per protected area is comparable.

Comparison of parameter influence on internal CP lifetime between different hotspots (WP A and WP B, linear and pw PC approach)
For internal GACP systems in WP B the critical spot lays at the upper MP part, below the TB. Sensitivity is studied at both spots, the critical one (TB) and at mudline (hotspot for internal GACP systems in WP A) to allow for different comparisons. Both wind farms have various anode designs and arrangements as well as different water depths and current requirements.
Figures A.7 to A.10 in Appendix A show the sensitivity study plots for linear and pw PC fittings for internal GACP systems in WP B.

- **Anode capacity ϵ:** Influence of anode capacity is equal for both WPs at both regarded spots for both approaches, linear and pw PC fitting.

- **Input anode potential E_{Al}:** E_{Al} shows for the linear case at the hotspot (TB) a continuously decreasing progress, whereas the pw approach at the hotspot as well as both approaches (linear and pw) at mudline show an inverse V-shape progress. Lifetime deviation is strongest for the pw case at the hotspot, but the linear case at mudline. Furthermore, the discussed cases in WP B do not show any similarities with WP A.

- **Seawater conductivity σ_{sea}:** The influence of seawater conductivity differs strongly at the critical spot (TB) between linear and pw case. In the linear case lifetime decreases with increasing σ_{sea}. For the pw curve lifetime runs down to zero for decreasing σ_{sea}. That can be explained by failure case 2, in which anode current does not reach the hotspot. The same is seen for the pw approach at the mudline, but not for the linear method. Here, the lifetime starts increasing again with decreasing σ_{sea}; failure 2 can be precluded. For rising σ_{sea} anodes start to deplete faster and therefore lifetime is decreasing.

- **Mud conductivity σ_{mud}:** Mud conductivity has nearly no influence on lifetime variations, which is seen from the horizontal curve progress in both analyzes (linear and pw PC fitting) at the hotspot. It should be noted here, that the hotspot at TB lays far away from the seabed, which might explain the low sensitivity. This proposition is strengthened by a steeper progress for the evaluated point close to the mudline, which is seen in Figure A.9 and A.10.

- **PC slope in mud i_{mud}:** The PC slope in mud shows in all cases for both wind farms the same progress as the respective mud conductivity in each case.

Concluding it can be said, that influence of seawater conductivity and anode potential are very inconsistent for all internal evaluations. An obvious pattern for influence on lifetime deviation is nearly unfeasible to generate. The reason for inconsistent results could be different designs and anode arrangements, which in turn would lead to an advise against comparing different CP designs. Another issue could be higher PC slopes, which were seen in all internal analyzes, but not externally. Consequently, it is recommended to treat predictions resulting from analyzes with small current requirements with caution, when outcomes are based on seawater conductivity and anode potentials.

Nonetheless, mud conductivity and PC slope in mud (i_{mud}) have similar effects in all regarded cases in both WPs, for internal and external GACP systems. Variations in anode capacity results in any case in the same progress. For parameters showing a similar sensitivity, like anode capacity, mud conductivity, and PC slope in mud, the simplified linear approach can be applied for reliable analyzes. In case of similar designs and environmental conditions results might be reliable for generalization.

4.1.3.2 Model Uncertainties: Influence of PC Slope i_{sea}

Lifetime resulting from varying i_{sea} values are evaluated to take model uncertainties into consideration, which might occur from PC fitting. To estimate on sensitivity of PC slope all other parameters are set to their bc. i_{sea} values are listed in Table 4.4. The regarded GACP system in WP A has internally a bc i_{sea} value of 0.05 A/m^2/V and externally of 0.01 A/m^2/V.

Table 4.4: Linear PC slope for worst, base, and best case in WP A and resulting normalized lifetime deviations.

		worst	**base**	**best**
internal	i_{sea}	0.095	0.05	0.005
	lifetime deviation	0.22	1	16.78
external	i_{sea}	0.025	0.01	0.001
	lifetime deviation	0.65	1	1.63

First of all it should be noted, that the design lifetime of the internal GACP system is about 5 times smaller than design lifetime of the regarded external CP systems; the bc lifetime internally (calibrated to environmental data and PC fitting to PoH measurements) is more than 40 times smaller than the external bc lifetime after PC fitting.

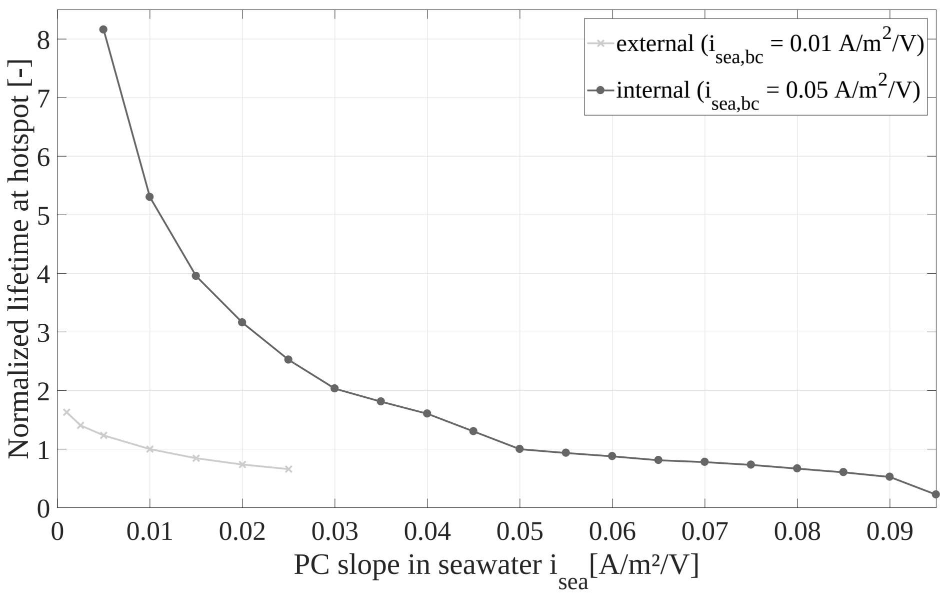

Figure 4.7: Normalized lifetime over variation of linear PC slope in WP A; externally with $i_{sea,ext}$ = 0.01 A/m^2/V (bright line) and internally with $i_{sea,int}$ = 0.05 A/m^2/V (dark line).

Figure 4.7 illustrates that the curve progresses around the respective bc externally and internally are similar regarding normalized lifetime deviation. However, absolute lifetime deviation is larger for external GACP, since the bc lifetime is already about 40 times higher.
The sensitivity around the absolute i_{sea} value of 0.01 A/m^2/V is much greater internally, which is seen by a steeper curve progress. This steep curve progress leads to higher normalized lifetimes for internal GACP systems when PC slope is 0.01 A/m^2/V.

For increasing PC slopes, internally and externally, the lifetime deviation curve is almost flat. The internal system lifetime would reach zero for an i_{sea} value of 0.1 A/m^2/V. External GACP lifetimes approaching zero would be expected for PC slope values 18.5 times higher than the bc ($>$ 0.185 A/m^2/V), which is not seen in Figure 4.7.
The influence of increasing PC slopes is less sensitive in lifetime deviations compared to decreasing PC slopes, for internal and external GACP systems. Thus, predictions on GACP systems show higher sensitivities in best case scenarios.

The variation in curve progresses between external and internal GACP systems can be explained by different anode designs, specification, and arrangements. In particular a huge difference between both GACP designs is the total initial anode mass and hence anode design lifetime. This shows, that comparison between different designs might be practically unfeasible. CP lifetime per anode mass should be critically questioned when designing CP systems.

Conclusively it can be said, that PC fitting analyzes for external CP systems result in lifetime prediction outcomes with smaller uncertainties, whereas outcomes from internal GACP evaluations should be regarded with high caution, especially in best case scenarios with small i_{sea} values.

4.1.4 Robustness of Results based on a Second Measurement Series

Data from second measurements one year later are analyzed and compared to results from the first year. This allows for statements about robustness of the PC fitting approach.
The potentials in both years are measured at three different elevations. It is assumed that measurement points in both years are equal and weather seasonality is neglected due to lacking environmental data. However, all on-site measurements are done between April and October and water temperatures as well as salinity, and with that seawater conductivity, can be assumed in similar ranges.

The following figures (Figure 4.8 and Figure 4.10) show measured potentials (x-axis) over height (y-axis) for external and internal GACP systems at two different measurement dates (year 1 and year 2). Year 1 is illustrated with black solid lines, year 2 with dashed gray lines. Potential differences between both years ΔE_{years}, calculated by Equation 4.1, are plotted in Figure 4.9 and Figure 4.11.

$$\Delta E_{years} = E_{WTG_{x,year\,1}} - E_{WTG_{x,year\,2}} \tag{4.1}$$

where:
$E_{WTG_{x,year\,1}}$ = potential at WTG x in year 1 $[V]$
$E_{WTG_{x,year\,1}}$ = potential at WTG x in year 2 $[V]$

Potential measurements from both years are available for external GACP systems at 13 WTGs and for internal systems at 16 turbines.

Comparison of external GACP measurements from two years

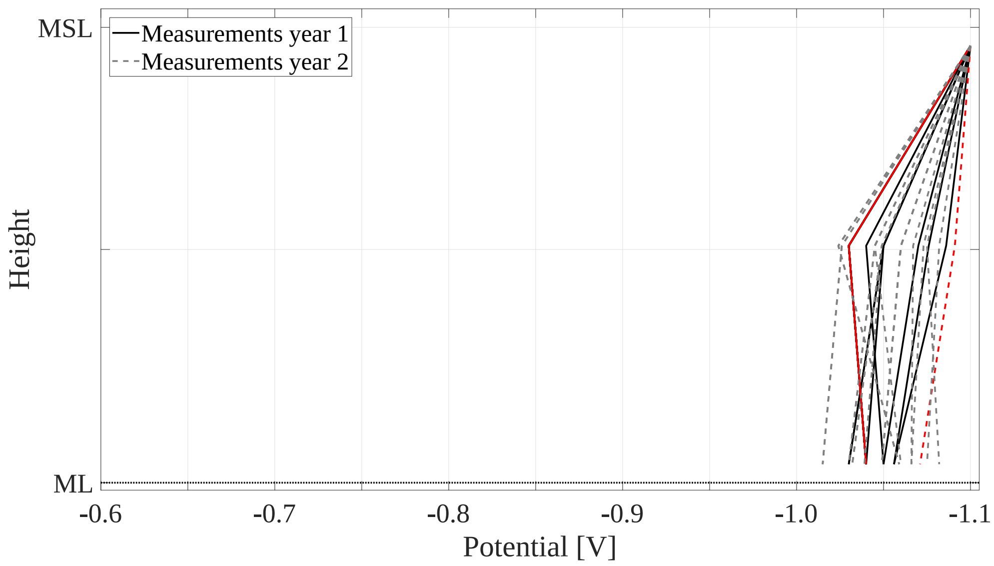

Figure 4.8: Protection potential range for 13 external GACP systems in WP B in year 1 (dark solid line) and year 2 (bright dashed line); red line: measurements with the largest difference between both years. The scatter is 0.085 V.

In Figure 4.8 it is clearly seen that variations in external GACP systems are small - especially at the upper measurement position, where all measurements are similar. This would validate, that the reference electrode measured the voltage very close to the anodes, which are located at the top, close to the upper measurement point.
The maximum variation between both years is 0.085 V and differs strongest from -0.025 to 0.06 V at the middle position, as seen in Figure 4.9. Around mudline the differences decrease slightly, which might be due to minor seawater currents around seabed. Furthermore, the measurement height can be better determined and are therefore less uncertain, when the reference electrode reaches the ground. Smaller differences at mudline could also be explained by the influence of the soil resistance, which has a more stabilized behavior over seasons and time. The stronger fluctuations at the middle elevation can be explained by e.g. a floating reference electrode (further away/closer to the MP surface) or uncertainties from varying protection

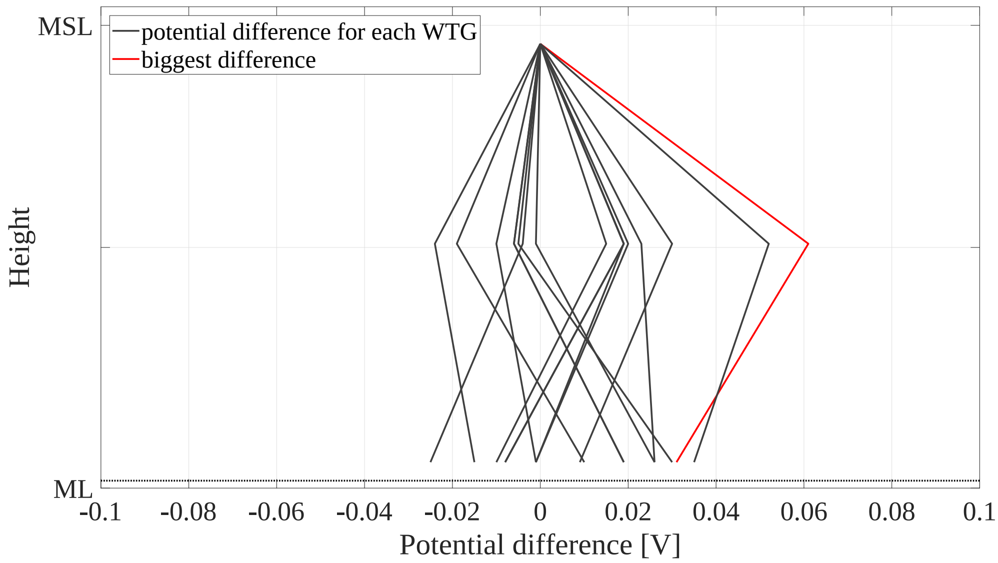

Figure 4.9: Potential difference for external GACP systems between two measurement years; red line: largest difference.

conditions. More negative potentials can e.g. occur due to a higher seawater conductivity (higher water temperature) or better performance of the calcareous deposit. Additionally, variations could occur from poor calibrated measurement equipment or measurement errors, which is however quite unlikely since measurements at the upper measurement elevation are all similar.
Evaluation of both measurements allow the conclusion, that external measurements look quite stable, even though the differences between the years are randomly either positive or negative. However, conditions are mostly stabilized and measurements one year later are comparable to the ones in the year before with variations of +/- 10%. PC fitting to three measurement points and hence lifetime predictions of external GACP systems are very similar for both years.
This conclusion is based on the assumption that measurement positions and environmental conditions are similar.

Comparison of internal GACP measurements from two years

As plotted in Figure 4.10 the range for all internal measurements in both years goes from -0.785 to -0.974 V. Figure 4.11 shows that the difference is in a large scatter from -0.058 to 0.096 V. At some locations potentials are more negative in year 1 but at others in year 2; around 75% of the regarded GACP systems have higher potentials in the second year (positive potential differences).
An overall evaluation of internal measurements shows that potentials are varying randomly between different turbine locations, measurement positions, and measurement dates. Several issues, like variations in pH value and calcareous deposit layer or water exchange in the inner MP, inaccurate measurements at different elevations. But also turbine specific changes in anode arrangement could be liable for inconsistent variations.

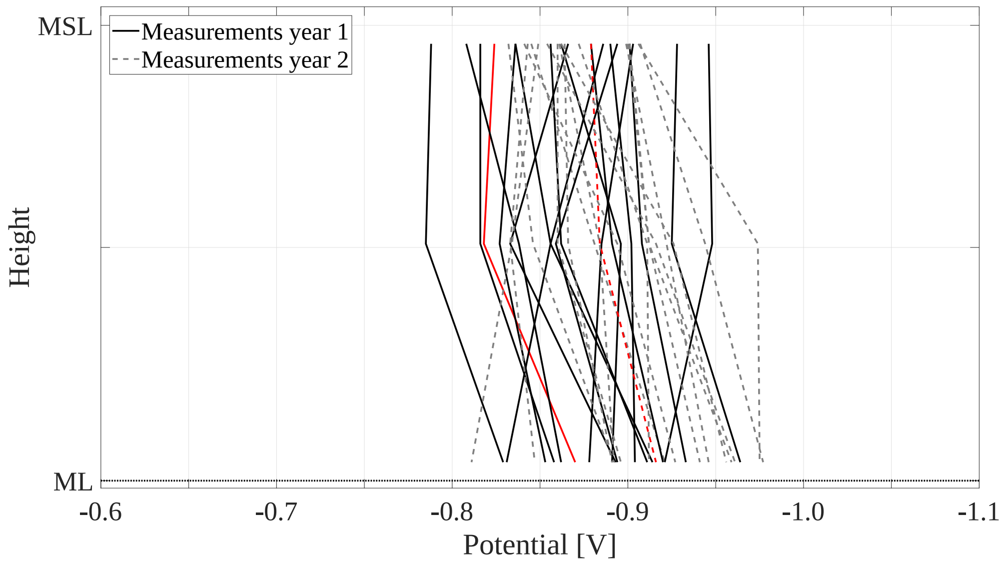

Figure 4.10: Protection potential range for 16 internal GACP systems in WP B in year 1 (dark solid line) and year 2 (bright dashed line); red line: measurements with the largest difference between both years. The scatter is 0.154 V.

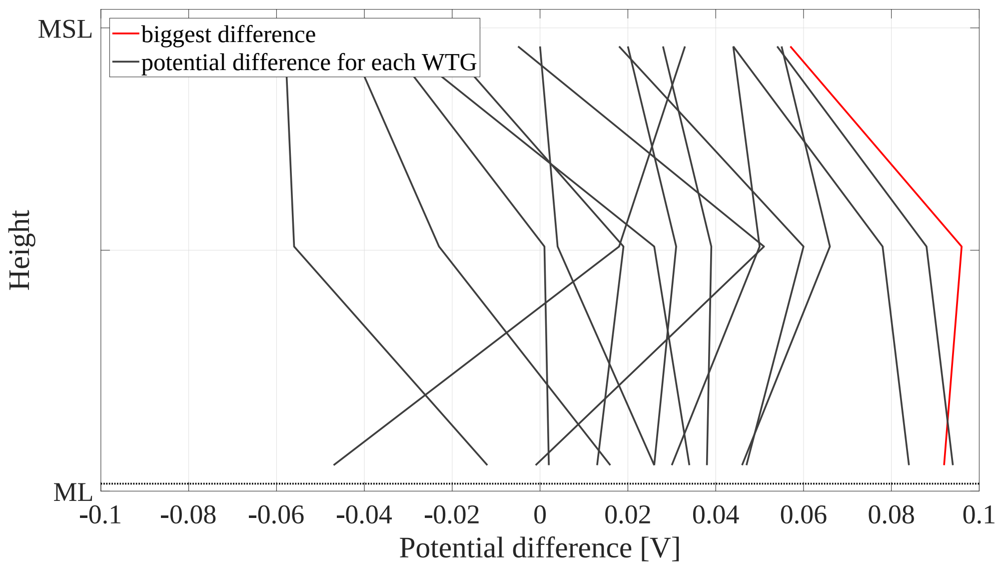

Figure 4.11: Potential difference for internal GACP systems between two measurement years; red line: largest difference.

Worst and best case comparison from a GACP system (at one WTG) between two years

To consider how robust results from internal measurement series are regarding CP lifetime, PC fitting and lifetime evaluation is performed for the turbines with the larges potential difference between both measurements. The approach introduced in Section 4.1.2 is applied.

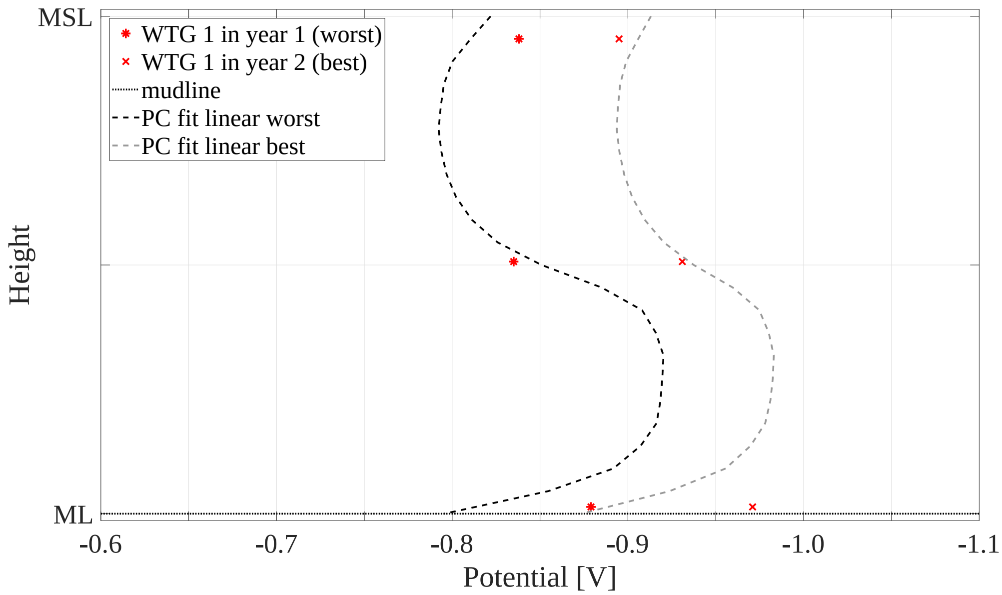

Figure 4.12: Two potential measurements at WTG 1 with linear PC fitting; year 1: worst case (dark line) and year 2: best case (bright line).

Figure 4.12 shows a PC fit for WTG 1 (fictitious notification) with a linear PC slope i_{sea} of 0.17 A/m^2/V in the first year. Whereas the PC fitting for the same turbine results in a slope of 0.07 A/m^2/V in year 2. This fluctuation of factor 2.4 and a difference in current requirements of 0.1 A/m^2 per volt protection potential indicates a low robustness of the applied method. One measurement per turbine and year at three measurement elevations can lead to results differing from a lifetime reduction by 98.3% (11.7% of bc lifetime) in year 1 to an increase of 3% from bc lifetime for linear PC fitting in year 2.
It should be noted, that protection potentials could also be better in year 1 and show worse protection in year 2 (negative differences, c.f. Figure 4.11).

An important modification would be to update design and measurement data in order to lower uncertainties. Furthermore, it is crucial to ensure accurate PoH measurements at exactly the same elevation and cross section point, especially when CP systems are not symmetrically. Several measurement elevations as well as consideration of MSL height and water depth at measurement dates would allow for more accurate PC fittings; robustness and certain statements about the developed method might be verified by improved measurements.

Furthermore, it is seen, that simulation and measurement points are difficult to properly match, especially when only three measurement points per OWT are regarded. A precise fit is unfeasible from the implemented model set-up and therefore results should be treated with caution.

4.2 ICCP

The data series from internal and external ICCP systems contain anode current output, voltage output, and potential measurements from the mounted reference electrodes. Data is available in 10 minutes time steps from several turbines over different time periods between November and July (in the following year). At all evaluated data series similar behavior is discernible over the time after settings are adjusted to stabilized conditions.

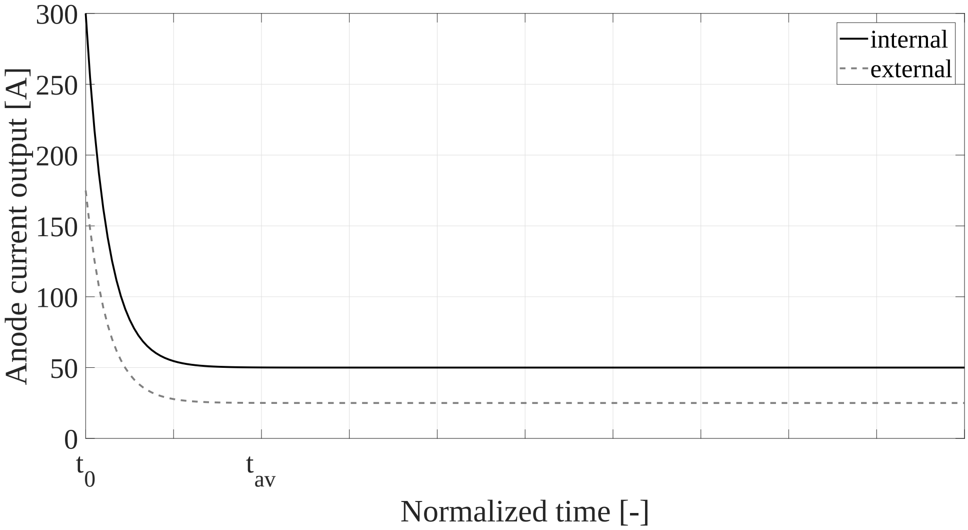

Figure 4.13: Anode current output over normalized time for an internal (dark solid line) and external (bright dashed line) ICCP system at one WTG in WP C.

Figure 4.13 shows the anode current output [A] over the normalized time, for an internal (dark solid line) and an external (bright dashed line) ICCP system after setting adjustments. The initial phase (t_0) implies the time when the ICCP systems are turned on and a very high current output is measured (values around 150 A for external to 300 A for internal ICCP systems). Due to a calcareous deposit build up, the current decreases in the first weeks until it stabilizes at t_{av}. The stabilized current output is around 25 A for external and 50 A for internal systems. The difference in external and internal current output can be explained by the distance from the anodes to the MP surface, which is larger inside the MP.

The supplied voltage shows a similar progress over time: very high in the initial phase and the mean stabilized value varies in between 3 V to 5 V for external and up to 10 V to 15 V for internal ICCP systems. In the data series the measured voltages show a large amount of outliers, jumping from 0 V to very high values around 50 V. Those oscillations might occur due to shut downs in periodic time intervals, which are needed to measure the potential by reference electrodes. Since potentials show a very stable progress, it is assumed that the ICCP system is controlled by potentials recorded from stationary reference electrodes. It should be noted here, that stationary reference electrodes, mounted close to the TB, are only be implemented to alert form overprotection. To ensure full protection over the whole MP and especially at the critical spot, manual measurements, like for GACP, must be undertaken.

If similar environmental conditions as for the wind farms with GACP systems and a full protection over the whole surface are assumed, the average current density reaching the structure can be estimated by Equation 3.3. For a mean value in the stabilized phase, the internal average current density would be 70 mA/m^2. Externally the average i_{sea} value would be 35 mA/m^2.
Both values are within the expected ranges (under the mentioned assumptions): 30 to 65% lower than the design requirements noted in codes.
A lower current density would allow for extended service life of the ICCP system, if underprotection is excluded at any point of the structure. As seen from the results, ICCP systems have large reserves of anode material and hence service life extension might be simple.
Possible seasonal changes of seawater conductivity are not recognized and information on coating was not implemented.

4.3 Significance for Monopile-based OWTs

A case study is performed to estimate on RUL at one hotspot (here: mudline), if CP fails before MP lifetime is reached. Stresses and SN-curves (for CP and FC) are again applied from studies by Ziegler [30] and are not related to any conditions at WP A, WP B, or WP C.

Case study: load data from *OC3* MP [30], hotspot: mudline
By means of Miner's Rule (c.f. Equation 2.11) the MP lifetime is calculate for x years cathodic protected plus the possible remaining lifetime under FC until a damage of 1 is reached.
Figure 4.14 illustrates the MP lifetime as a function of CP system service life in years. If no CP shields the surface at the mudline, fatigue failure is expected to occur after 6.49 years, which is more than 3 times shorter as the design lifetime of the MP; usually MP design lifetimes are around 20 to 25 years. Since D is a cumulative sum, the remaining time a MP suffers from FC is decreasing with increasing CP lifetime (until D = 1). The total MP lifetime is extending linear, since D_{CP} is smaller than the D-value for free corroding metal surfaces.
The maximum total lifetime at mudline is 32.89 years until fatigue failure occurs (no FC).

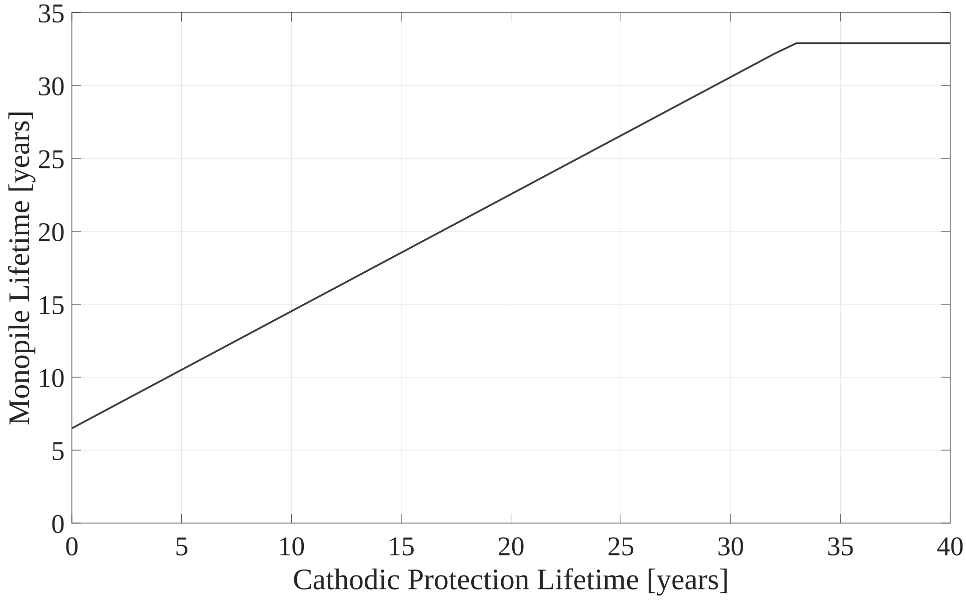

Figure 4.14: MP lifetime as a function of service life of a CP system in years for a **case study** with a minimum MP lifetime of 6.49 years and a maximum MP lifetime of 32.89 years.

It should be noted here, that analyzes with other load cases and at different spots lead to changing lifetime outcomes. The influence of coating is neglected in the performed case study.

4.4 Limitations

The applied method to evaluate service time of CP systems is based on several assumptions and simplifications. Nevertheless, the evaluated outputs give a proficient review of possible prolonged lifetime of CP systems by evaluating on-site measurements and simulation outcomes. Results are based on data provided from three different wind farms and cannot be generalized. For practical implementation each case must be considered in particular, depending on external conditions and influences. Some assumptions are not unavoidable due to missing data or experiences, others are just simplifications to provide an efficient implementation of the thesis' scope and requirements. In the following list main limitations are mentioned:

1. **Measurement uncertainties**
   Repeatability of the approach is difficult due to high measurement uncertainties leading to a large scatter of PC fitting possibilities. Thus, precise predictions on CP lifetime are not easily reliable.

2. **Location specific environmental parameters**
   Evaluated results regard only corrosion control in North Sea conditions. In other waters and in mud-containing electrolytes chemical composition and en-

vironmental parameters might differ and therefore the PC progress and with that results would also change.
Several data was missing or generalized in the presented method, but should be adjusted manually for each study, ideally by actual on-site data.

3. **Parameter sets for sensitivity study**
   Parameter ranges are chosen based on literature, experiences, and expert opinion. For the sensitivity study the parameters are assumed to be independent from each other. A global sensitivity analysis would allow for consideration of parameter interaction.

4. **Failures in CP systems and structure**
   The methodology only applies for turbines without damages and failures on turbines. Performance of CP systems is investigated for two failure cases: (1) anode depletion and (2) anode current is unable to reach all points at the MP surface.

5. **General simplifications in geometry model**
   The simulation model is built as a simplified MP structure. Models must be adjusted for different wind farms and turbines. Secondary steel parts are neglected in this study. Impact on service time of the MP due to damages on secondary steel parts are not considered, but can influence LTE decisions. Jackets or other marine structures with complex surfaces have to be evaluated with adjusted approaches providing uniform protection potentials in each edge and joints.

6. **Results below mudline**
   A lack of measurements in soil leads to simplified soil conditions, based on data from codes. The real potential distribution below the mudline can only be assumed based on experiences and simulations. Therefore, results close to mudline should be interpreted with caution.

7. **Coating and coating breakdown factor**
   Implementation of different coating types and with that varying coating breakdown factors is excluded in this thesis. The coating breakdown factor is only included for the mean case performing according to design assumptions, but should be time-dependent in reality.
   The area of the coated part is modified to design reports, but varies between locations and measurement date due to changing MSLs.

8. **Uncertainties in seawater and seabed levels**
   Protected MP surface changes from different seawater levels, as well as varying mudline depths due to location specific reasons like soil push-up and scour. Simulation should be adapted if precise data are available.

9. **Neglection of MIC**
MIC is neglected in this study, due to missing literature and experiences. To account for MIC more negative protection potentials might be necessary. The question on how to deal with MIC at OWTs can be addressed in future works.

10. **Influence from chemical parameters**
The corrosive effect due to chemical parameters, except of salinity, is neglected. Special caution should be given on the effect of pH value and calcareous formation. The 'tertiary current distribution model' in COMSOL Multiphysics® allows for individual input of chemical parameters.

11. **Limited number of regarded turbines**
The method is applied at one or two turbines per wind park. Individual analyzes for each turbine location should be performed to allow for quantitative lifetime predictions for each position.

12. **SN-curve analysis**
LTE analyzes are only applied for case studies based on data from Ziegler [30]. Real on-site load data is needed to estimate on structure lifetime at the regarded wind farms.

13. **Re-polarization neglected (stabilized PC curve)**
This study only regards the case of a stabilized PC over the whole lifetime. A possible re-polarization after a storm event or any other reasons for a breakdown of the stabilized conditions might result in poorer lifetime predictions and should be evaluated in future works.

14. **Constant conditions over lifetime**
It is assumed, that all conditions (environmental parameters, PCs, etc.) and designs (anode and steel potentials) are stabilized and stay constant over the evaluated time and future. In reality environmental data are time and season dependent and thus, PC might change over time.

4.5 Industrial Implementation and Scientific Value

For industrial application LTE of OWTs becomes crucial, and therefore performance of corrosion control systems must be estimated. In order to analyze CP systems in a cost-efficient approach industry could profit from practical application due to:

- evaluation of service life of CP system, which is required by codes [1] to predict on LTE for MP,
- assessment on CP systems, if lifetime of CP is shorter than MP lifetime (usually internal) to decide on replacement of anodes,
- design improvements of CP systems for new wind farm projects (regarding anode distribution), and

- recommendations on measurement approaches regarding importance of environmental parameters as well as PoH measurements.

The question whether industry application is reliable cannot be answered in this thesis. The stated limitations show that practical implementation of the presented methodology should be treated with caution and decisions should always taken fact-based. Furthermore, an improvement of measurements is highly recommended to allow on sufficient estimations on service life extension. However, an initial investigation follows from the developed approach, showing how simulation can be applied for corrosion control purposes and how sensitivity and representativeness of measurement data looks like.

The scientific novelty of that study was to evaluate, whether estimations on CP lifetime are reliable by fitting different kinetic expressions in corrosion simulation models to on-site measured potentials.

4.6 Social, ethical and ecological Aspects

Wind energy, as a renewable energy source, is nowadays a crucial part of the energy mix to meet the energy demand worldwide. Since, the first OWFs are reaching the end of their design lifetime soon, extended operating time becomes increasingly important. Lifetime extension will not only reduce costs, but can also avoid renaturation, planning, and investment of new wind farms.
Corrosion is one aspect to be considered, when it comes to the question whether LTE of OTWs is feasible.

Furthermore, corrosion itself is addicted with economic, health, and safety problems. Corrosion, which is the irreversible loss of metal can be a big issue for structural fatigue failure. The deterioration of metal structures due to corrosion are fraught with high uncertainties. This can lead to a high health and safety risks for the environment. It should be also noted here, that corrosion protection systems like coatings and sacrificial anodes can emit substances which might be harmful or toxic for the environment as well as for humans. Those aspects should be considered when designing corrosion control system for OWTs.

5

Conclusion and Recommendations

LTE becomes very appealing, since the first OWFs will reach the end of their design lifetimes soon. Corrosion protection plays a significant role on structural behavior regarding bearable stresses. Development of a cost-efficient approach by modifying simulations with available potential and environmental measurements would lead to a huge benefit for wind farm operators.
The crucial question of corrosion in the context of LTE for monopile-based OWTs was mentioned in the problem statement:

Is there a possibility for prolonged service life of cathodic protection systems for further estimations on lifetime extension of monopile-based offshore wind turbines?

This work devised an approach to estimate on lifetime of CP systems by modification of simulation models with measurement data. The following core elements are applied:

- interpretation of on-site measurement data for simulation calibration and further interpretation of post-processing analyzes,
- set-up of kinetic expressions by means of iterative simulation adjustment based on PoH measurements (PC fitting),
- estimations on PC performance with regard on robustness and sensitivity, and
- application for service life predictions of offshore MPs.

The investigated methodology of fitting PC to PoH measurements showed, that current requirements for external GACP systems are 10 times smaller than design values, which is surprisingly small. That, in turn would result in a high increase of GACP service life. Simulation of internal GACP systems illustrated current requirements in the same range or higher than in the design. Furthermore, a large scatter in lifetime predictions, especially for internal GACP systems, indicated that results are afflicted with high uncertainties.
A comparison of simulation outcomes for two different dates at one internal GACP system resulted in lifetime deviations of -98.3 to +3%. Externally variations in PoH measurements were minor.
PC fitting illustrated that simulation outcomes from studies with a simplified PC slope (linear) are similar to results from simulation with pw PC slopes, mainly for external GACP systems.

In both GACPC systems, externally and internally, the sensitivity to mud conductivity and current drain in soil is small; especially in cases where mudline is deep, influence of soil conditions are nearly negligible regarding lifetime variations of (external) GACP systems. Reductions in seawater conductivity can lead to missing corrosion protection for internal designs, although anode material is not completely depleted. Variations in anode potential show high sensitivities for lifetime deviation (from 0 to 115%) even though value range is small (-1.0 to -1.1 V). Hence, special attention should be paid on measuring and determining on those parameters to further apply in simulations.

Model uncertainties as well as irregularities in measurement data lead to a low robustness of the applied method for lifetime predictions of internal systems, whereby analyzes of external CP performance are less sensitive to variations in PoH measurements and thus in PC changes.
Recapping it can be said, that precise measurements should be performed to confirm CP simulation outcomes with higher representativeness and to allow for accurate PC fittings, which can thus be used to specifically predict on lifetime of CP systems.

This study indicated on top, that simulation provide additional information on corrosion protection design considering anode arrangement and deviation over the structure as well as location of the critical spot. This lead to the conclusion, that CP design is of major importance and estimations on CP lifetime is infeasible to generalize one-to-one to other offshore wind projects.

Nonetheless, the developed methodology contains initial estimations of assessment on CP systems and their performance and might be applied for maintenance planning. Uncertainties and low representativeness inescapably leads to the need of pursued investigations. First notions on an enhanced method to estimate on corrosion protection are mentioned in the following paragraph.

By measuring the current output from CP systems, lifetime of anodes could be estimated directly and compared to simulations and design. However, potential measurements are necessary to eliminate underprotection at any part of the structure, especially at critical hotspots, even though anodes are still existing. Data from anode current output in combination with potential measurements would lower uncertainties for PC fitting drastically. Furthermore, visual inspections would provide sufficient knowledge about MP and anode conditions, e.g. whether deposit layers and marine growths are formed on MP surfaces or to gauge on anode size.

Coupons, with a metallic behavior similar to the MP surface or anode material, can be mounted in a way to allow a later disassembly. Removed coupons can be inspected in laboratories and allow on determination of the corrosion rates.

Recommendations for future works

This thesis contributes to a better understanding of the complexity of corrosion control for offshore applications in wind industries and how measurements and simulations can be applied for corrosion protection predictions to meet code requirements on LTE for OWTs.

Future work is needed to strengthen robustness and to allow for higher representativeness of measurements implemented to adjust simulation models. The following recommendations are defined for future development in academics and industry:

1. **Implementation of more measurement data**
   Additional measurement data, e.g. potential measurements in soil, but also environmental parameters like seawater current or chemical compositions and pH value would lead in improved understanding of CP behavior under particular conditions.
   For practical implementations at existing OWFs simulations must be adjusted to environmental and location specific conditions. Individual information for each measurement date and location as well as detailed continuous measurements would lead to huge benefits.

2. **Modification of simulation model and corrosion kinetics**
   The geometry model applied for simulation was built as a simplified structure, which could be enormously improved by detailed computer aided design structures. Additional input parameters can be complemented and modified, like the implementation of a time dependent coating breakdown factor to account for degradation of the coating over service time.
   Corrosion kinetic expression (also for anodes) can be further studied, in theory and practical implementation for offshore substructures, to allow for more realistic and precise PCs in each phase.

3. **Improvement of sensitivity study**
   Uncertainties are only assessed for several parameters based on expert opinion. Additional sensitivity studies are recommended to account for all parameter variations. Furthermore, a global sensitivity analyzed would consider interaction between parameters and lead to important details for further improvement.

4. **Generalization of work**
   To generalize the work's approach estimations on CP systems for other support structures can be accomplished. Ancillary studies for ICCP systems would lead to additional information on corrosion control and benefits in experiences for future applications.
   Methods for corrosion protection systems, e.g. coating, for new wind farm projects should be developed to consider possible LTE already in an early stage of design.
   Furthermore, MIC will have an important influence on the possibilities of extending service life of the CP and is recommended to evaluate in future works.

5. **Corrosion monitoring strategy**
   To allow for representative predictions on CP system lifetime, a detailed monitoring strategy should be developed, e.g. including current output measurements and an improvement of potential measurement as well as monitoring of residual anode mass.

6. **Cost evaluation and reliability**
   Development of an economic model that allows cost estimates for corrosion control of extending lifetime is strongly advised, if it comes to practical implementation in industries. This model should additionally help deciding on optimal methods for corrosion control reassessments.

Bibliography

[1] DNV GL. ST-0262: Lifetime extension of wind turbines. *Standard*, 2016.

[2] Carlos Guedes Soares, Yordan Garbatov, A. Zayed, and G. Wang. Influence of environmental factors on corrosion of ship structures in marine atmosphere. *Corrosion Science*, 51(9):2014–2026, 2009.

[3] DNV. RP-B401: Cathodic Protection Design. *Recommended Practice*, 2010.

[4] Lisa Ziegler, Sven Voormeeren, Sebastian Schafhirt, and Michael Muskulus. *Sensitivity of wave fatigue loads on offshore wind turbines under varying site conditions*, volume 80. Elsevier B.V., 2015.

[5] Seth Price and Rita Figueira. Corrosion Protection Systems and Fatigue Corrosion in Offshore Wind Structures: Current Status and Future Perspectives. *Coatings*, 7(2):25, 2017.

[6] DNV GL. RP-C203: Fatigue Strength Ananlysis of Offshore Steel Structures. *Recommended Practice*, 1(c):246–253, 1981.

[7] DNV. OS-J101: Design of Offshore Wind Turbine Structures. *Offshore Standard*, pages 212–214, 2014.

[8] Maria Martinez Luengo and Athanasios Kolios. Failure Mode Identification and End of Life Scenarios of Offshore Wind Turbines: A Review. *energies*, 8:8339–8354, 2015.

[9] Lisa Ziegler and Michael Muskulus. Fatigue reassessment for lifetime extension of offshore wind monopile substructures. *Journal of Physics: Conference Series*, 753:092010, 2016.

[10] Lisa Ziegler and Michael Muskulus. Lifetime extension of offshore wind monopiles: Assessment process and relevance of fatigue crack inspection. *EAWE PhD Seminar*, 12th:1–5, 2016.

[11] Jutta Stutzmann, Lisa Ziegler, and Michael Muskulus. Fatigue Crack Detection for Lifetime Extension of Monopile-based Offshore Wind Turbines. *Energy Procedia*, (To Appear).

[12] Andreas Momber. Corrosion and corrosion protection of support structures for offshore wind energy devices (OWEA). *Materials and Corrosion*, 62(5):391–404, 2011.

[13] Andreas Momber, Peter Plagemann, Volkmar Stenzel, and Michael Schneider. Beurteilung von Korrosionsschutzsystemen für für Offshore-Windenergietürme – Teil 2: Ergebnisse und Schlussfolgerungen. *Stahlbau*, 78(6):394–401, 2009.

[14] Karsten Hempel. Corrosion Protection for Windmills. pages 1–12, 2004.

[15] Oliver Heins. Korrosionsschutz von Offshore-Windenergieanlagen. 2011.

[16] Force Technology. Corrosion protection of offshore wind farm structures – present understanding and future challenges. pages 1–9, 2011.

[17] Arnaud Meillier. A review of galvanic anode cathodic protection design procedure. *Journal of Corrosion Science and Engineering*, 4:1–29, 2003.

[18] William H. Hartt, S. Chen, and D.W. Townley. Sacrificial Anode Cathodic Polarization of Steel in Seawater: Part 2 — Design and Data Analysis. *Nace International*, CORROSION(4):317–322, 1998.

[19] William H. Hartt and S. Chen. Galvanic Anode Cathodic Polarization of Steel in Seawater: Part III — Retrofit Cathodic Protection of Offshore Structures. *Nace International*, CORROSION:596–605, 1999.

[20] William H. Hartt. Path dependence of the potential-current density state for cathodically polarized steel in seawater. *Corrosion*, 56(1):3–11, 2000.

[21] William H. Hartt and E. Lemieux. A Principal Determinant in Cathodic Protection Design of Offshore Structures — The Mean Current Density. *Nace International*, CORROSION:988–997, 2000.

[22] William H. Hartt. Cathodic protection of offshore structures - history and current status. *Corrosion*, 68(12):1063–1075, 2012.

[23] DNV GL. RP-0416: Corrosion protection for wind turbines. *Recommended Practice*, 2016.

[24] BSH. Mindestanforderungen für den Korrosionsschutz an Offshore-Anlagen in der Ausschließlichen Wirtschaftszone (AWZ) von Nord- und Ostsee. 2013.

[25] BAW. Guidelines for the testing of coating systems for the corrosion protection of hydraulic steel structures. (January):24, 2001.

[26] BAW. Kathodischer Korrosionsschutz im Stahlwasserbau (MKKS). *BAW Merkblatt*, 2015.

[27] NACE. Standard Test Method Measurement Techniques Related to Criteria for Cathodic Protection of Underground Storage Tank Systems. (21231), 2012.

[28] NACE SP0176. Corrosion Control of Submerged Areas of Permanently Installed Steel Offshore Structures Associated with Petroleum Production. *Standard Practice*, (21018), 2007.

[29] ASTM. Standard Practice for Calculation of Corrosion Rates and Related Information. *Standard Practice*, 89(Reapproved):1–7, 1999.

[30] Lisa Ziegler, Sebastian Schafhirt, Matti Scheu, and Michael Muskulus. Effect of Load Sequence and Weather Seasonality on Fatigue Crack Growth for Monopile-based Offshore Wind Turbines. *Energy Procedia*, 94:115–123, 2016.

[31] Pierre R. Roberge. *Handbook of Corrosion Engineering*. 1999.

[32] Gerald S. Frankel. *Active Protective Coatings*, volume 233. 2016.

[33] Junming Ho, Michelle L. Coote, Christopher J. Cramer, and Donald G. Truhlar. Theoretical Calculation of Reduction Potentials. *Organic Electrochemistry*, 2015.

[34] W. von Baeckmann, W. Schwenk, W. Prinz, and Editiors. *Handbook of Cathodic Corrosion Protecion*. 1997.

[35] Milton Stern. The electrochemical behavior, including hydrogen overvoltage, of iron in acid environments. *J. Electrochem. Soc.*, 102(11):609–616, 1955.

[36] Howard A. Perko. Corrosion and Life Expectancy. *John Wiley & Sons*, pages 295–323, 2009.

[37] B. Kermani and L.M. Smith. *A Working Party Report on CO2 Corrosion Control in Oil and Gas Production: Design Considerations*. Number 23. 1997.

[38] NORSOK M-501. Surface preparation and protective coating. *Norsok Standard*, page 32, 2012.

[39] DS/EN ISO 12944-1. Maling og lak – Korrosionsbeskyttelse af stålkonstruktioner med maling – Del 1: Generel introduktion / Paints and varnishes – Corrosion protection of steel structures by protective paint systems – Part 1: General introduction. *Dansk standard*, 2, 2004.

[40] ISO 20340. Malinger og lakker – Ydeevnekrav til korrosionsbeskyttende malings- systemer til offshorekonstruktioner / Paints and varnishes – Performance requirements for protective paint systems for offshore and related structures. *International Organization for Standardization / Danish Standards Foundation*, page 34, 2009.

[41] Herbert H. Uhlig. Effect of local-action currents on the iron potential. pages 276–285, 1953.

[42] Yuanfeng Yang, James Scantlebury, and Elena Koroleva. A Study of Calcareous Deposits on Cathodically Protected Mild Steel in Artificial Seawater. *Metals*, 5:439–456, 2015.

[43] Mars Fontana. *Corrosion Engineering*. 1987.

[44] J. L. Solis and J. Genesca. Effect of Calcareous Deposit Formation on Galvanic Anode Cathodic Protection of Steel in Seawater. *Nace International Conference & Expo*, (09520):1–10, 2009.

[45] Marinela Panayotova, Yordan Garbatov, and Carlos Guedes Soares. Corrosion of steels in marine environment, monitoring and standards. *Safety and Reliability of Industrial Products, Systems and Structures*, pages 369–412, 2010.

[46] DS/EN ISO 8044. Korrosion af metaller og legeringer – Grundlæggende termer og definitioner / Corrosion of metals and alloys – Basic terms and definitions. *Dansk standard*, 2015.

[47] Norio Sato. Basics of Corrosion Chemistry. In *Green Corrosion Chemistry and Engineering: Opportunities and Challenges*, pages 1–32. 2011.

[48] COMSOL Multiphysics®. Corrosion Module Application Library Manual, 2016.

[49] COMSOL Multiphysics®. Introduction to the Corrosion Module, 2016.

[50] COMSOL Multiphysics®. Corrosion Module, 2016.

A

Appendix A

A.1 Convergence study for model set-up

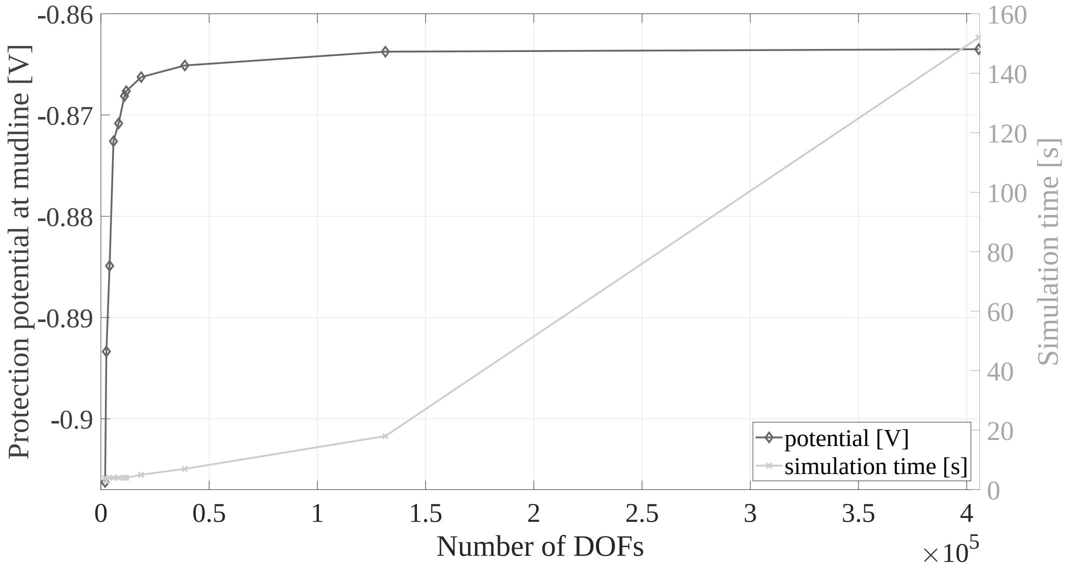

Figure A.1: Meshing of the electrolyte: Protection potential [V] at one point of MP surface (left y-axis; dark line) and simulation time [s] for stationary case (right y-axis; bright line) over number of DOFs.
Converged after 10,890 DOFs (COMSOL default mesh) within the set accuracy of 0.005 V; simulation time for one stationary case: 4 s.

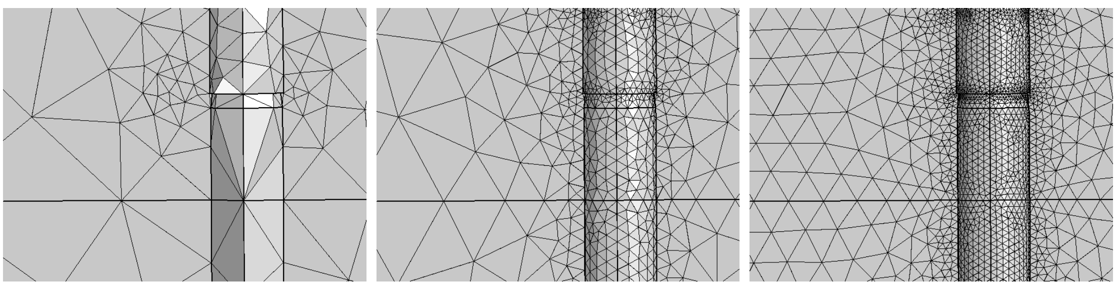

Figure A.2: Electrolyte mesh around a schematic MP structure: extremely coarse (DOF = 1940), default (DOF = 10,890), extremely fine (DOF = 131,413).

A.2 PC fitting for GACP systems in WP B

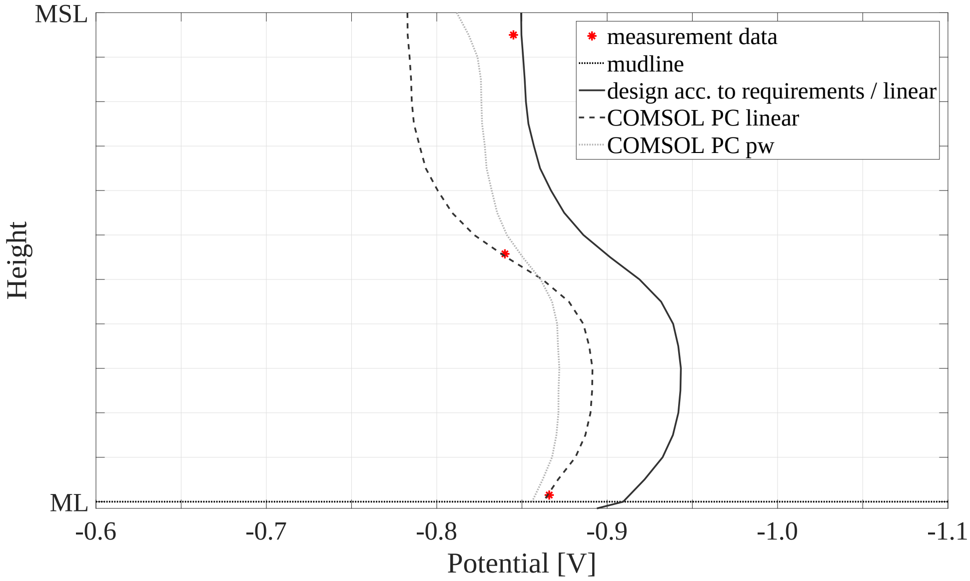

Figure A.3: PC fit for an **internal** GACP system in WP B to measurement data (red dots); design PoH progress for linear PC slope (dark solid line) according to requirements and after model calibration and PC fitting to measurement data with PC slopes: **(a) linear** (dark dashed line), **(b) pw** (bright dashed line).

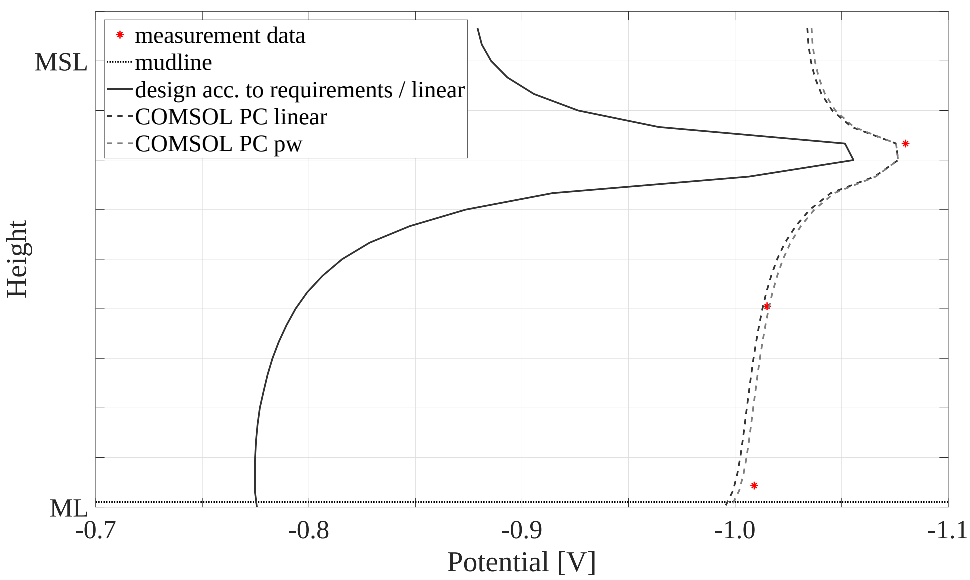

Figure A.4: PC fit for an **external** GACP system in WP B to measurement data (red dots); design PoH progress for linear PC slope (dark solid line) according to requirements and after model calibration and PC fitting to measurement data with PC slopes: **(a) linear** (dark dashed line), **(b) pw** (bright dashed line).

A.3 Sensitivity of external GACP in WP B

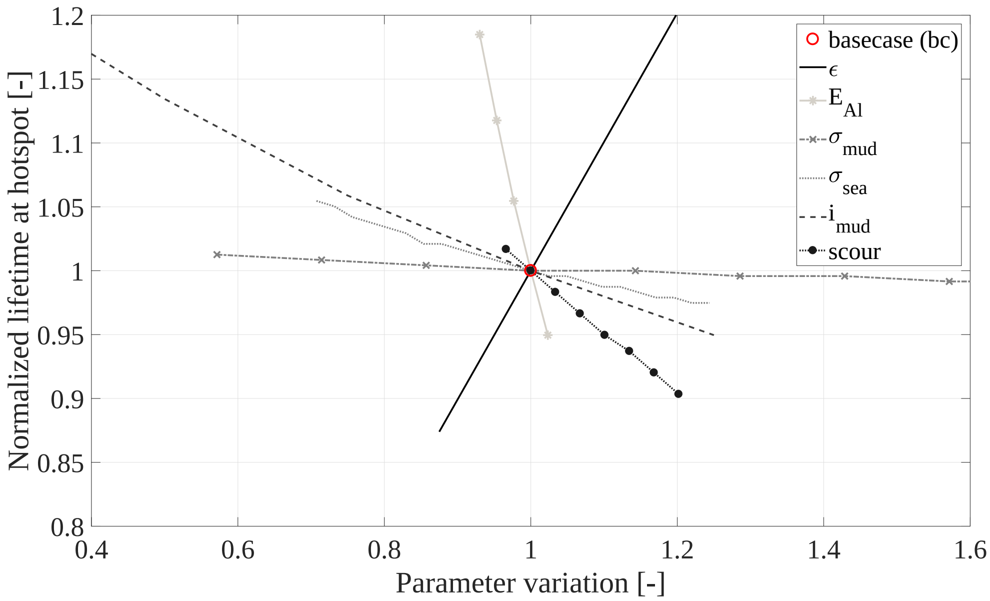

Figure A.5: Normalized lifetime over parameter variations at the hotspot (here: mudline) of an external GACP system in WP B with **(a) linear** PC slope.

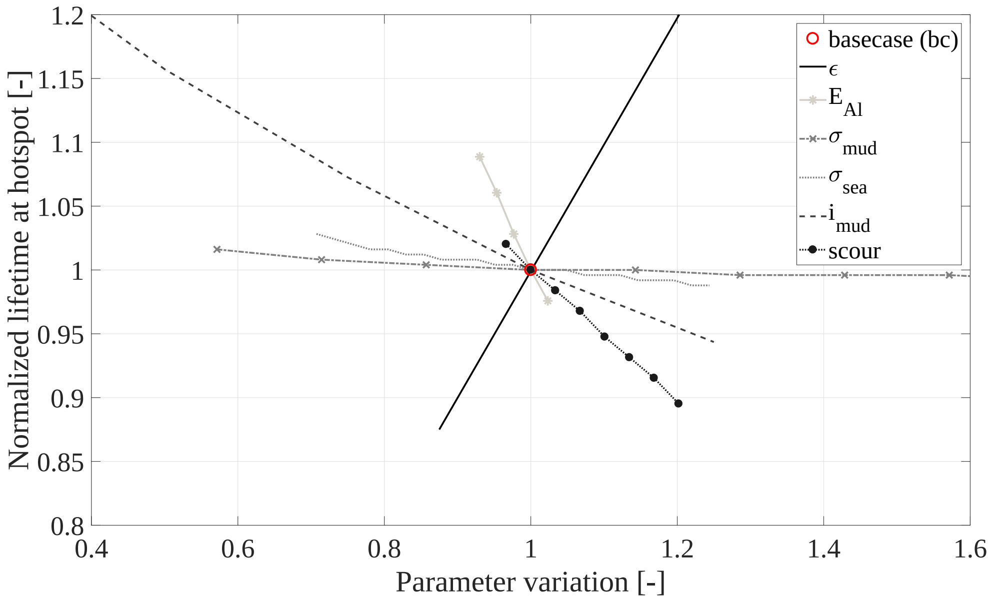

Figure A.6: Normalized lifetime over parameter variations at the hotspot (here: mudline) of an external GACP system in WP B with **(b) pw** PC slope.

Table A.1: Input parameters for worst, base, and best cases for an external GACP system in WP B with **(a) linear** and **(b) pw** PC slope.

Parameter	**Unit**	**bc**	**(a) linear**		**(b) pw**	
			worst	**best**	**worst**	**best**
E_{Al}	V	-1.075	-1.1	-1.0	-1.1	-1.0
ϵ	Ah/kg	2000	1750	2750	1750	2750
σ_{sea}	S/m	4.1	5.1	2.9	5.1	2.9
σ_{mud}	S/m	0.7	1.5	0.4	1.5	0.4
i_{mud}	$A/m^2/V$	0.02	0.025	0.005	0.025	0.005
Scour	m	0	-6	+1	-6	+1
Lifetime deviation	-	1	*N/A**	*N/A**	*N/A**	*N/A**

**N/A: no calculation performed*

A.4 Sensitivity of internal GACP in WP B

Sensitivity at hotspot

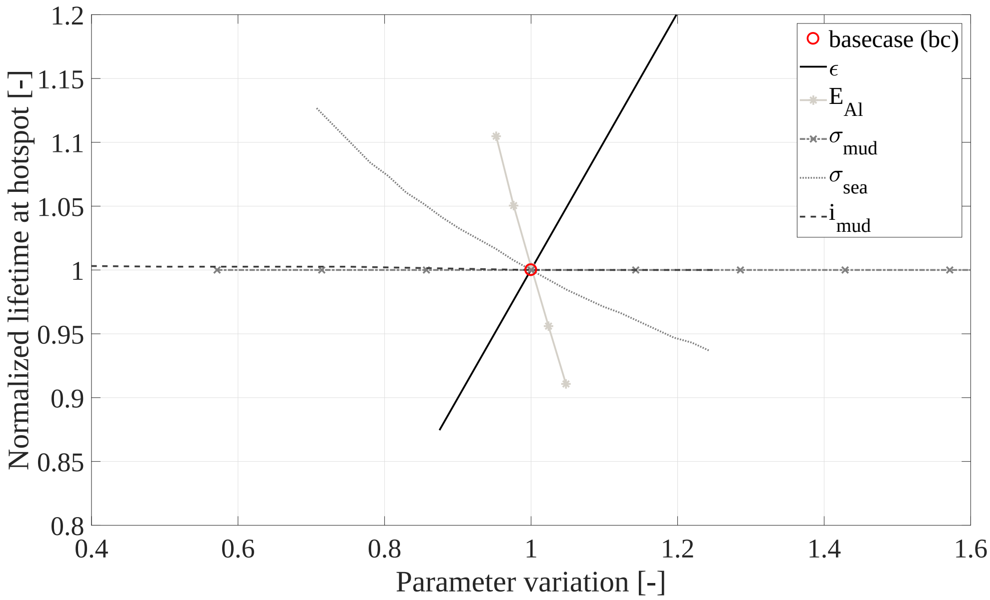

Figure A.7: Normalized lifetime over parameter variations at the hotspot (here: below TB) of an internal GACP system in WP B with **(a) linear** PC slope.

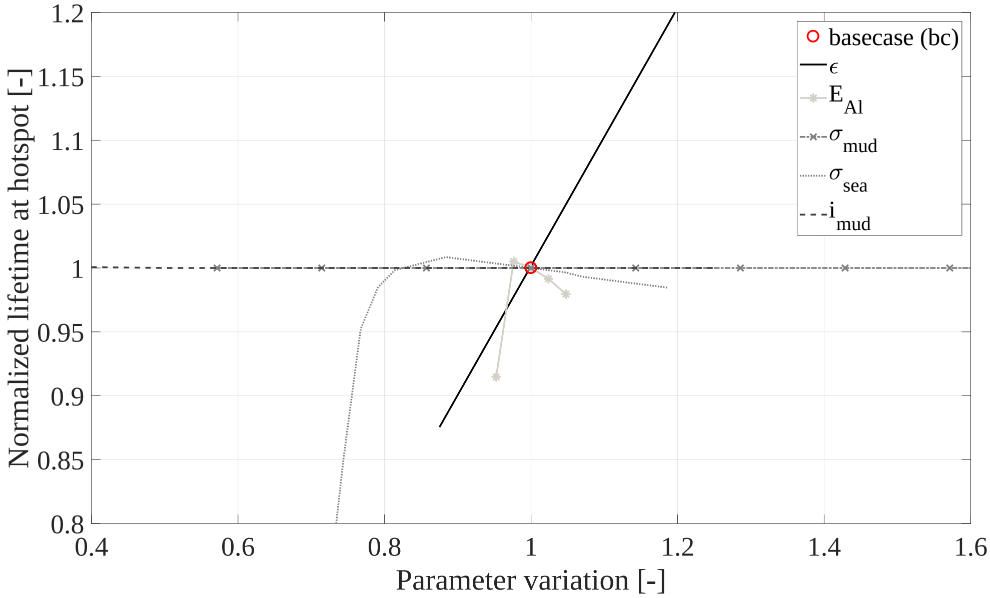

Figure A.8: Normalized lifetime over parameter variations at the hotspot (here: below TB) of an internal GACP system in WP B with **(b) pw** PC slope.

Table A.2: Input parameters for worst, base, and best cases for an internal GACP system in WP B at hotspot (here: below TB) with **(a) linear** and **(b) pw** PC slope.

Parameter	**Unit**	**bc**	**(a) linear**		**(b) pw**	
			worst	**best**	**worst**	**best**
E_{Al}	V	-1.05	-1.1	-1.0	-1.0	-1.025
ϵ	Ah/kg	2000	1750	2750	1750	2750
σ_{sea}	S/m	4.1	2.9	5.1	2.9	3.8
σ_{mud}	S/m	0.7	1.5	0.4	1.5	0.4
i_{mud}	$A/m^2/V$	0.02	0.025	0.005	0.025	0.005
Lifetime deviation	-	1	*N/A**	*N/A**	*N/A**	*N/A**

**N/A: no calculation performed*

Sensitivity at mudline

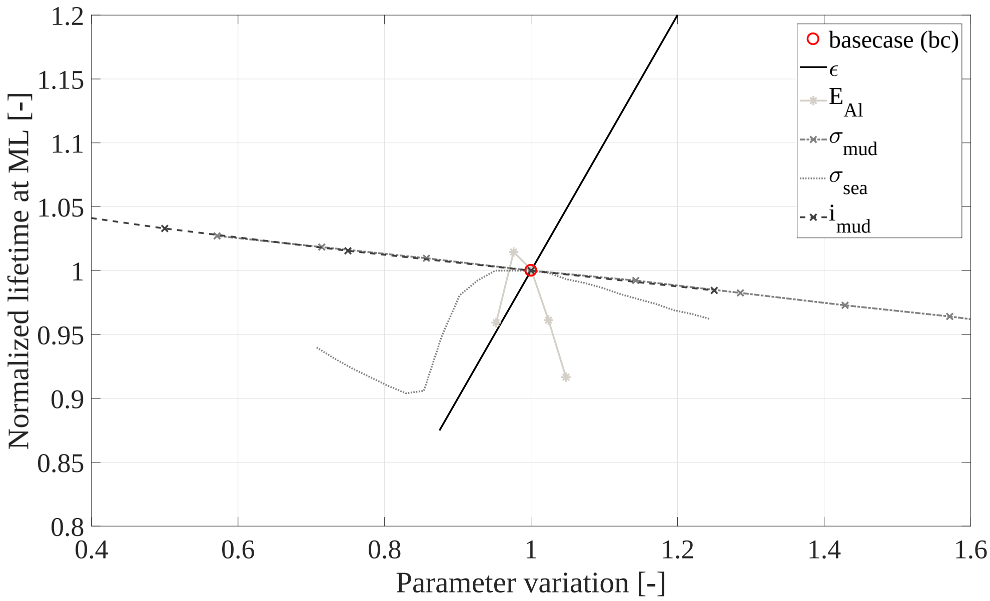

Figure A.9: Normalized lifetime over parameter variations at mudline of an internal GACP system in WP B with **(a) linear** PC slope.

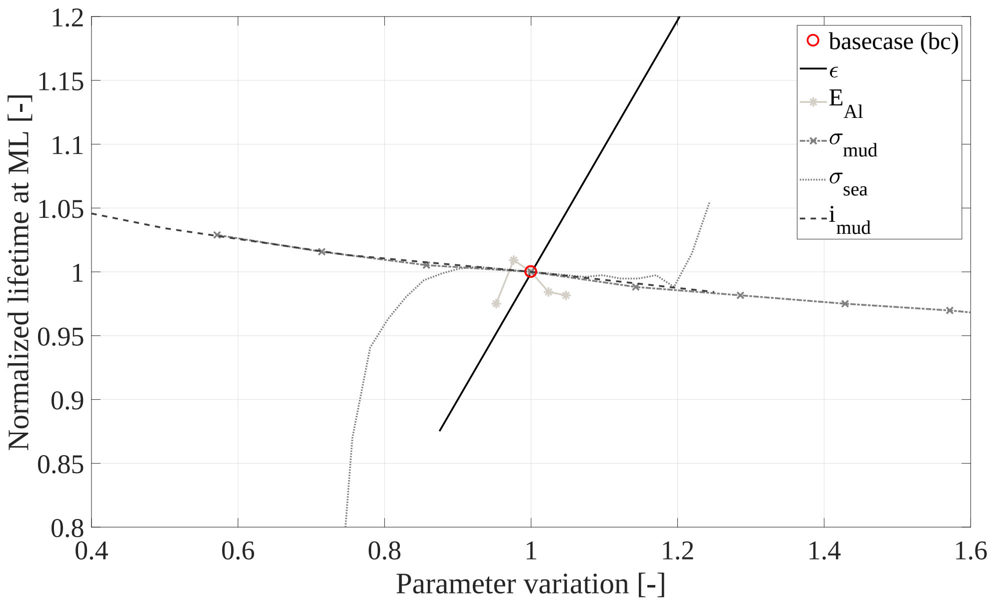

Figure A.10: Normalized lifetime over parameter variations at mudline of an internal GACP system in WP B with **(b) pw** PC slope.

Table A.3: Input parameters for worst, base, and best cases for an internal GACP system in WP B at mudline with **(a) linear** and **(b) pw** PC slope.

Parameter	**Unit**	**bc**	**(a) linear**		**(b) pw**	
			worst	**best**	**worst**	**best**
E_{Al}	V	-1.05	-1.1	-1.0	-1.0	-1.025
ϵ	Ah/kg	2000	1750	2750	1750	2750
σ_{sea}	S/m	4.1	3.4	5.1	2.9	5.1
σ_{mud}	S/m	0.7	1.5	0.4	1.5	0.4
i_{mud}	$A/m^2/V$	0.02	0.025	0.005	0.025	0.005
Lifetime deviation	-	1	*N/A**	*N/A**	*N/A**	*N/A**

**N/A: no calculation performed*